STRUCTURAL AND STRATIGRAPHIC AGE CONSTRAINTS OF THE INSKIP FORMATION, EAST RANGE, NEVADA: IMPLICATIONS FOR MESOZOIC TECTONICS OF WESTERN NORTH AMERICA

By

Joshua David Wilkins

A thesis

submitted in partial fulfillment

of the requirements for the degree of

Master of Science in Geology

Boise State University

December 2010

BOISE STATE UNIVERSITY GRADUATE COLLEGE

DEFENSE COMMITTEE AND FINAL READING APPROVALS

of the thesis submitted by

Joshua David Wilkins

Thesis Title: Structural and Stratigraphic Age Constraints of the Inskip Formation, East Range, Nevada: Implications for Mesozoic Tectonics of Western North America

Date of Final Oral Examination: 27 September 2010

The following individuals read and discussed the thesis submitted by student Joshua David Wilkins, and they evaluated his presentation and response to questions during the final oral examination. They found that the student passed the final oral examination.

Clyde J. Northrup, Ph.D.	Chair, Supervisory Committee
Walter S. Snyder, Ph.D.	Member, Supervisory Committee
Mark D. Schmitz, Ph.D.	Member, Supervisory Committee

The final reading approval of the thesis was granted by Clyde J. Northrup, Ph.D., Chair of the Supervisory Committee. The thesis was approved for the Graduate College by John R. Pelton, Ph.D., Dean of the Graduate College.

ABSTRACT

Structural, stratigraphic, and U-Pb geochronologic studies of the Inskip Formation of the north-central East Range place new constraints on the depositional age of the Inskip Formation and the timing of contractional deformation in the East Range, including Golconda thrusting. The Inskip Formation was initially considered Permian in age and to rest unconformably on the Valmy (or Leach) Formation (Ferguson et al., 1951). Later mapping by Whitbread (1978, 1994) divided the formation into the Upper and Lower Inskip Formation, both of which were inferred to be Mississippian in age. Later reinterpretation of Whitebread's (1994) work and new paleontological data revised the age of the Inskip Formation as Permian through the Devonian, and interpreted the Upper and Lower Inskip Formation as facies of the Havallah sequence (Ketner et al., 2000, 2008). The current study retains the use of Upper and Lower Inskip Formation for discussion and their use as distinct tectono-stratigraphic units; however, the new data from the study have led to a significantly revised interpretation of what the units represent.

The Lower Inskip Formation is reinterpreted to be structurally above the Valmy Formation (Silberling, 1962; Hargett, 2002) and unconformably overlain by the Upper Inskip Formation. The Lower Inskip Formation contains arkosic sandstone, conglomerate, phyllite, siliceous argillite, quartzite, minor shale and limestone, and some greenstones. Fossils from the Lower Inskip Formation have yielded ages ranging from Pennsylvanian to the Devonian (Ketner et al., 2000; Hargett, 2002). This study assigns

the Lower Inskip Formation to the Havallah sequence. In contrast, Siberling et al. (1962) only assigned the northern most section of the Inskip Formation to the Havallah sequence and separated it from the rest of the Inskip Formation by a thrust fault, and Ketner et al. (2000) assigned the entire Inskip Formation to the Havallah sequence.

The Upper Inskip Formation lies unconformably over the Lower Inskip Formation and contains amphibolite/greenstone, phyllite, and quartzite, with lesser amounts of limestone and some felsic volcanic deposits. Only one fossil has been identified in the Upper Inskip Formation and it yielded an age of Permian (Ketner et al., 2000). However, new U-Pb zircon geochronology of a tuff (sample 08JW534) collected in the Upper Inskip Formation yielded an age of Early Triassic (249.08 +/- 0.14 Ma). Due to the new radiometric age control and similarity of lithostratigraphy, the Upper Inskip Formation is correlated with the Limerick Member of the Koipato Group.

The Golconda Thrust places upper Paleozoic Havallah sequence basinal rocks on top of lower Paleozoic rocks of the Roberts Mountains allochthon and its overlap sequence, while the Koipato Group rests unconformably on the Havallah sequence (Silberling et al., 1962). With the new age data and assignment of the Lower Inskip Formation to the Havallah sequence and the Upper Inskip Formation to the Limerick Member, the same relationship exists in the north-central East Range as in northern Tobin Range where the Sonoma orogeny was originally recognized (Silberling et al., 1962). Therefore, the contact between the Lower Inskip Formation and the Valmy Formation is interpreted to be a portion of the Golconda Thrust, which is considered the basal thrust of the Sonoma orogeny.

At least five phases of deformation occurred in the Upper and Lower Inskip Formation of the East Range. The first phase of deformation (D_1) formed the angular unconformity between the Inskip Formation and the Rochester Member. The second phase (D_2) included thrusting of Early Triassic rocks and upper Paleozoic rocks of the Havallah basin over the lower Paleozoic rocks of the Roberts Mountains allochthon. D_3 formed the penetrative foliation, which is prevalent throughout the area. The fourth phase of deformation (D_4) resulted in map scale folding, including the large northeast-southwest trending antiform across the north-central East Range. The fifth phase (D_5) produced SE-vergent folding throughout the area and a crenulation cleavage in the less competent phyllite and along some of the western limbs of these folds. The age of the entire deformational sequence is constrained to have occurred between the last depositional event (the Upper Inskip Formation), which has an age of Early Triassic (249.08 +/- 0.14 Ma), and the intrusion of relatively nondeformed late Middle Jurassic sills (161.80 +/- 0.04 Ma). The timing and structural style of deformation exhibited in (D_5) appears very similar to that resulting from the Fencemaker fold and thrust belt (Oldow et al., 1984; Speed et al., 1989; Wyld, 2002). Deformation in the East Range and the Sonoma Range are interpreted here as expressions of Mesozoic contraction, kinematically linking the Luning-Fencemaker and the Golconda thrust systems.

TABLE OF CONTENTS

LIST OF TABLES

LIST OF FIGURES

LIST OF PLATES

INTRODUCTION

The East Range of north-central Nevada is situated in an important structural position with respect to Late Paleozoic-Mesozoic contractional orogenesis in the North American Cordillera, in that it contains traces of the Golconda (southern East Range) and Fencemaker (northwestern) thrust faults through the East Range (Figure 1). Between the two thrusts lays the Winnemucca Fold and Thrust Belt of the northern Sonoma Range, and the Willow Creek Thrust in the north-central East Range. The stratigraphic ages, contact relationships, and structural evolution in the area are controversial and have been interpreted in contrasting ways by various authors. Upper Paleozoic rocks in the central East Range have been metamorphosed and penetratively deformed, obscuring the nature of the contacts between different units. Furthermore, relatively few datable fossils have been obtained from these units, making age control and correlation difficult.

The East Range is located at the western edge of exposure of Lower Paleozoic rocks from the Roberts Mountains allochthon. These rocks include the Valmy Formation, part of the basinal, and slope rocks of the Western Assemblage of Roberts et al. (1958). Also present are Upper Paleozoic rocks from the Golconda allochthon, represented by the Havallah sequence. Additionally, rocks from the Koipato Group are exposed in the East Range and represent Triassic volcanic and sedimentary rocks deposited unconformably over the Upper Paleozoic rocks.

Most of the rock units of the East Range can be correlated with those in other Mountain ranges adjacent to the East Range. The Inskip Formation, however, which has been divided into Upper and Lower subunits (Whitbread, 1978), is found only in the East Range. It has no previously identified equivalent in the surrounding area, and its relationship to other units is uncertain. The purpose of this study is to utilize geologic mapping, structural analysis, and U-Pb geochronology to better constrain the depositional age of the Inskip Formation and evaluate its significance in the regional tectono-stratigraphic framework. In addition, this study will analyze the structural and deformational history of the north-central East Range and determine the timing of major deformational events.

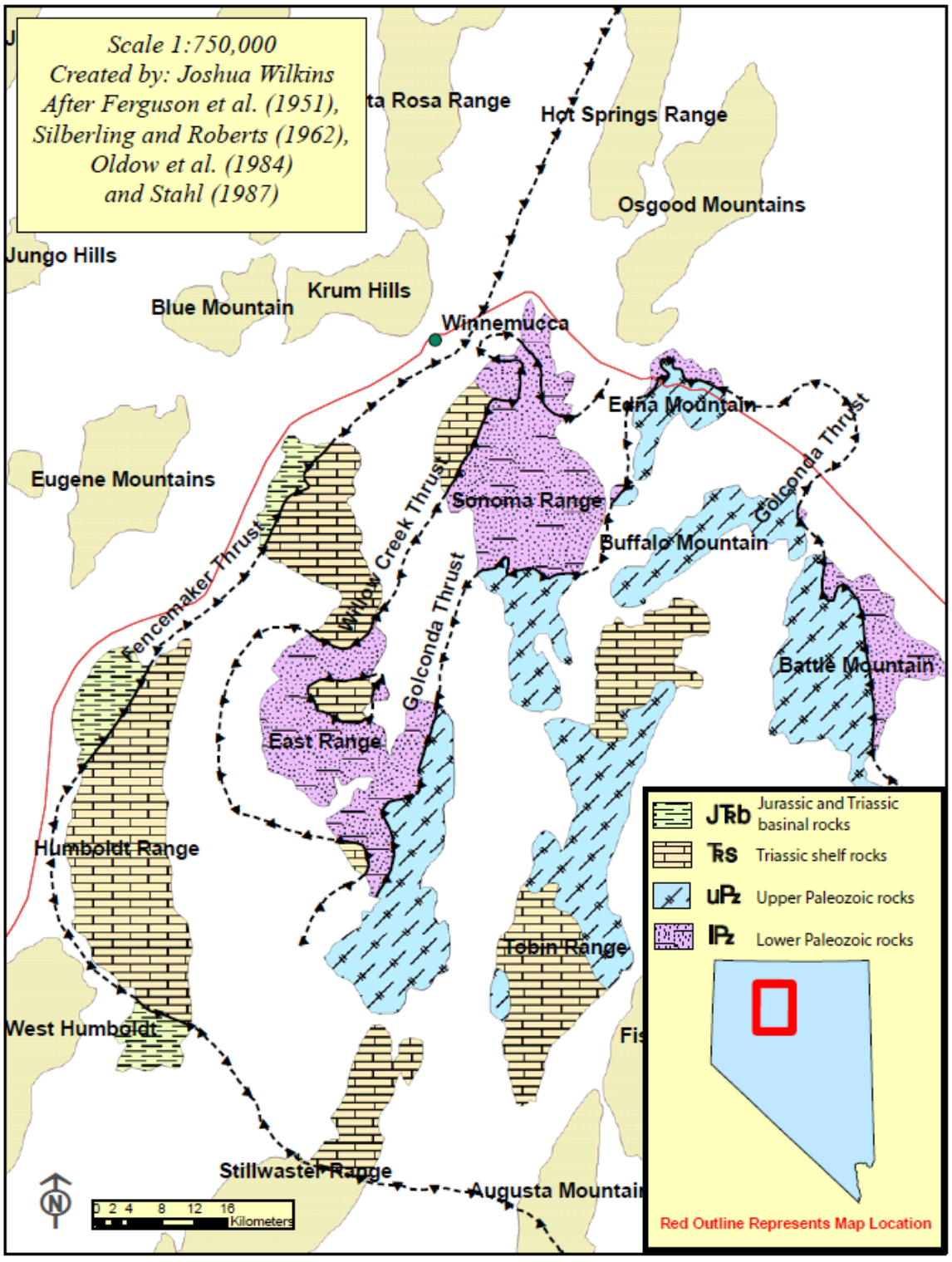

Figure 1. Simplified Geological Map of North-Central Nevada Showing Location, Age and Type of Rock, and Major Thrust Faults in Area.

GEOLOGIC FRAMEWORK

To provide context for the new data and interpretations, a synopsis of regional tectonic evolution is provided.

Antler Orogeny

Near the end of the Proterozoic (~600-550 Ma), the western edge of the North American craton (all directions are given in today's reference frame) established a passive margin setting known as the miogeocline (Speed et al., 1988; Burchfiel et al., 1992). In what is now eastern Nevada, an extensive carbonate assemblage over 3 km thick developed on the eastern shelf of a newly formed basin. Sedimentation continued until the Mississippian (Silberling and Roberts, 1962). Rifting prior to this time opened the oceanic basin and initiated the passive margin. The margin remained quiescent until deep marine rocks were thrust over shallow marine rocks of the continental margin during the Antler orogeny of Late Devonian to Early Mississippian time (~375-345 Ma) (Roberts et al., 1958; Burchfiel et al., 1992). During the passive interval before the Antler orogeny, the miogeocline developed a thick clastic wedge reaching thicknesses of 6 km and more (Burchfiel et al., 1992). The Valmy Formation Quartzite (Ordovician) was deposited in the clastic wedge on the continental margin. Also, the Harmony Formation was deposited as a large sub marine fan, generally considered Cambrian in age. The Harmony Formation was deposited in deeper water than the Valmy Formation Quartzite (Schweickert and Snyder, 1981). The Harmony Formation consists of feldspathic

sandstone that appears to have grading that could represent transport from relatively large distances via density currents (Silberling and Roberts, 1962).

The Antler orogeny of Late Devonian to Early Mississippian time thrust oceanic rocks and rocks from the clastic wedge that developed on the continental margin onto the miogeocline along the Roberts Mountains Thrust. The age of the Antler orogeny is constrained by deformed Devonian rocks being unconformably overlain by non-deformed Early Mississippian “overlap” sequence deposits (Roberts et al., 1958). Greenstone, pelagic, and hemi-pelagic sediments, quartzite, and turbidites were all incorporated in the overriding thrust plate (Roberts Mountains allochthon). Some researchers have suggested that a relatively small slice of continental crust had been rifted from the North American continent and may have provided a western source of the detrital component of the oceanic basin (Burchfiel et al., 1992; Poole and Sandberg, 1977). Evidence for the slice of continental crust come from arkosic sandstone deposits sourced to the west of the basin as well as detrital zircon studies showing a tie to the North American continent. An island arc (Klamath-Northern Sierra arc?) may have developed in association with the rifted slice of continental crust, with thrusting on the western side of the arc suggesting eastward directed subduction (Burchfiel et al., 1992). Additional evidence comes from the Valmy and Vinini Formations, which contain quartz grain that vary from coarser in the west to finer in the east (Roberts et al., 1958).

Reversal of arc polarity to westward directed subduction is presumably responsible for the closure of the basin and obduction of the Roberts Mountains allochthon onto the miogeocline of western North America (Burchfiel et al., 1992). However, no remnant arc is preserved adjacent to the Roberts Mountains allochthon.

Several theories have been developed to explain the absence of the arc: first, after accretion to the continental margin, the arc could have cooled, subsided, and been covered by younger sedimentary rock or later thrusts (Speed et al., 1988); second, there could have been an incomplete closure of the basin; and third, the arc could have been rifted away from the margin some time after accretion.

Evidence supporting a cooled and subsided arc has not been documented in the literature. Speed et al. (1988) suggested that the arc may have been completely subducted during the Sonoma orogeny. Alternatively after accretion, a new subduction zone may have formed to the west of the arc, and removed the heat source, allowing the arc to cool and subside (Speed and Silberling, 1989).

The second scenario, a partial closure of a basin during accretion of the Roberts Mountains allochthon, is supported by the fact that arc rocks have not been described structurally or stratigraphically adjacent to the Roberts Mountains allochthon. In this case, contraction may have stopped before obduction of arc rocks onto the continental margin.

The final theory, arc-continent collision followed by rifting to cause separation of the arc from the emplaced Roberts Mountains allochthon, is supported by several lines of evidence. The Klamath Mountains and the northern Sierras have long been known to have arc affinities, and they include rocks with ages that are analogous with ages obtained from rocks within the Roberts Mountains allochthon. If rifting focused along the accreted subduction complex, then an absence of arc rocks adjacent to the Roberts Mountains allochthon is not unreasonable. Additionally, rocks of similar character, dark grey vitreous quartzite, have been found adjacent to and east of the arc rocks in the

Klamath Mountains (locally known as the Vinini Formation). Rocks of the Valmy Formation represent the same type of quartzite within the Roberts Mountains allochthon (Schweickert and Snyder, 1981). The Valmy Formation and Vinini Formation could represent parts of the subduction complex accreted during the Antler orogeny, which later were separated by back-arc spreading and rifting.

At the end of the Antler orogeny, a belt of mountains extending from southern Idaho into southern California were left as a topographic high. This orogenic belt is known as the Antler highlands, and it shed clastic material to form the Antler overlap sequence (Roberts et al., 1958). Although termed "highlands," the Antler Mountains of northwestern Nevada were probably still submerged (Silberling and Roberts, 1962). Clastic material was transported up to 100 miles to the west and not as far to the east, with carbonate deposition continuing east of the Antler highlands (Roberts et al., 1958). Middle Pennsylvanian is the oldest uncontested age for rocks in the Antler overlap sequence (Roberts, 1964; Crafford, 2008).

Sonoma Orogeny

The next major tectonic event was the Sonoma orogeny of latest Permian to earliest Triassic time (Silberling and Roberts, 1962). Rocks deformed by this orogeny are contained within the Golconda allochthon, and were deposited in an ocean basin or a marginal back-arc basin setting. This basin has been termed the Havallah basin, with fossil ages for the rock units ranging in age from the Late Devonian to Permian. Although most of the Golconda allochthon consists of Carboniferous Havallah sequence, it also includes rocks as old as late Devonian, overlapping in age the rocks of the Roberts

Mountains allochthon (Burchfiel et al., 1992). The Havallah Basin may have been west of the Antler highlands where, during the Antler orogeny, the volcanic arc should have been. Or the Havallah basin rocks could have been thrust over a subsiding arc or several smaller basins could have been created within the arc even during the emplacement of the Roberts Mountains allochthon. Silberling and Roberts (1962) noted that the age of the Antler overlap sequence and the Havallah basinal rocks are the same, but their facies are significantly different. Therefore, a thrust with large transport distance would be required to bring the two into juxtaposition.

The Havallah basin was either an extensional back-arc basin or an open ocean basin floored by oceanic crust. Continued extension allowed for episodes of basaltic magmatism preserved in the Golconda allochthon as greenstones and pillow basalts. Some of the sediments deposited in the Havallah basin were derived from the Antler highlands and others were derived from a volcanic source to the west. Arc debris and plutonism were incorporated or intruded into sedimentary rocks of the Havallah sequence during a period of active volcanism between 252-267 Ma as recorded in the southern Havallah basin and Northern Sierras (Burchfiel et al., 1992). The volcanism and plutonism may have been derived from the same arc source (Burchfiel et al., 1992).

The Antler and Sonoma orogenies are strikingly similar in their manner of structural development and types of lithologies involved in the accretionary process (Brueckner and Snyder, 1985). One major similarity is the lack of a co-eval arc terrane adjacent to the emplaced allochthons. Both orogenies thrust oceanic rocks consisting of pelagic, hemi-pelagic, and mafic volcanic rock onto the continental margin of western North America.

The Sonoma orogeny was originally defined based on relationships in the Hoffman Canyon area of the Tobin Range of north central Nevada (Silberling and Roberts, 1962). At this location, Havallah sequence rocks (Carboniferous to Permian) are strongly deformed and unconformably overlain by weakly deformed rocks of the Triassic Koipato Group. Thus, an orogenic event occurred in the interval between Late Permian and Early Triassic. Because the strongly deformed rocks of the Havallah sequence had been structurally thrust over the older Roberts Mountains allochthon and its overlap sequence, the thrusting event has been interpreted as part of the Sonoma orogeny and assigned an age of Permian-Triassic. The Roberts Mountains allochthon and its overlap sequence have been over thrust by rocks originally deposited in the Havallah basin along the Golconda Thrust. Some researchers interpret the Golconda allochthon to be the subduction complex of an east-facing arc that consumed and closed the Havallah basin (Speed, 1977; Speed et al., 1988; Brueckner and Snyder, 1985). As the continental margin entered the subduction zone, the subduction ceased and final emplacement of the allochthon occurred (Burchfiel et al., 1992). Triassic rocks of the Koipato Group were then unconformably deposited on the Golconda allochthon. However, the Koipato Group only exists depositionally on the Havallah sequence rocks and does not extend across the Golconda Thrust onto the rocks of the Roberts Mountains allochthon or its overlap sequence. Because the Koipato Group rocks do not depositionally overlap the contact between the Roberts Mountains allochthon and the Golconda allochthon, the possibility exists that the Koipato Group rode “piggy-back” on top of the Havallah sequence and was part of the Golconda allochthon during emplacement (Burchfiel et al., 1992). If this

is the case, then the age of the Golconda thrust and the significance of the Sonoma orogeny would need to be re-evaluated.

Other authors have suggested an even younger age (Mesozoic) for the final emplacement of the Golconda allochthon and the conclusion of the Sonoma orogeny (Snyder and Bruckner, 1983; Ketner, 1984; Snyder and Bruckner, 1989; Dunston et al., 2001). The Quesnellia and Stikinia arc terranes were accreted to the continental margin of southern Canada during the middle Jurassic between 180-160 Ma (Burchfiel et al., 1992), which could have provided a driving mechanism for Mesozoic Golconda thrusting.

If the volcanism that produced the Koipato Group was the result of the westward subduction of the ocean or back arc basin beneath the volcanic arc, then the Koipato Group volcanics may date the final closure of the basin as early Triassic (Burchfiel et al., 1992). Localized extension was induced in the overriding plate while thrusting occurred near the eastern-most edge (Burchfiel et al., 1992). The arc presumably never overrode the continental margin, and thrust emplacement was limited to the basin deposits incorporated into the accretionary wedge, with the arc passively accreting after westward subduction had ended (Burchfiel et al., 1992).

An active margin developed off the western edge of the continent during Early Triassic time and remained for approximately 150 million years following the Sonoma orogeny (Speed et al., 1988). On the western side of the Klamath arc, an eastward dipping subduction zone had been re-established after the closure of the Havallah basin. The western Klamaths and rocks of Cache Creek affinity are interpreted to be an accreted subduction complex, an interpretation supported by the presence of blueschists of Late Triassic age (Burchfiel et al., 1992).

Early Triassic igneous activity has been documented over a wide spread area in central Nevada and into the Nevada-California border area. The total volume of rock, however, is relatively small (Saleeby and Busby-Spera, 1992). Pulses of magmatism also occurred with peaks from 165-155 Ma and 80-70 (Speed et al., 1988). This magmatism was derived from beneath the foreland of the continental arc, which had been established to the west (Speed et al., 1988).

Star Peak/Luning Basin

Although accreted during the Sonoma orogeny, the Golconda allochthon and much of the terrane between it and the eastern Klamath arc was covered by a relatively deep epicontinental sea (Burchfiel et al., 1992). This sea was the depositional environment for a volcanic source to the west, hemi-pelagic sedimentation, and turbidites in the deeper part of the basin. Near the eastern margin, the sea had shelf and deltaic deposition, which graded eastward into a continental depositional environment (Burchfiel et al., 1992). This basin is known as the Star Peak/Luning basin and was the site of active deposition until deformation associated with the Nevadan orogeny in the Middle Jurassic caused uplift and a cessation of sedimentation.

Rocks of the Star Peak/Luning basin consist mainly of mudstone, carbonate turbidites, and phyllite, with some siltstone and sandstone (Speed and Silberling, 1989; Wyld, 2002). Hemi-pelagic deposition of clay minerals was the source for the shale and phyllite. Turbitides likely brought the siltstones and sandstones into the deeper parts of the basin where they were interbedded with the shale and phyllite. Deformation near the area of Blue Mountain of north central Nevada produced a cleavage striking to the north-

east and dipping to the north-west (Oldow et al., 1984; Wyld, 2002). The penetrative cleavage is typically exhibited in the shale and phyllite, and may be the product of Early-Middle Jurassic deformation (Wyld, 2002). Vergence of folding is to the southeast (Oldow et al., 1984). Another deformational event created a crenulation cleavage with a north-east contraction that cut across the primary foliation and local folding (Oldow et al., 1984; Wyld, 2002). This second deformational event includes more brittle failure than the first, higher-temperature and more ductile event (Wyld, 2002).

A region including the Santa Rosa range to the northern East Range and westward to Jungo Mountain exhibits deformation similar to the area near Blue Mountain: a north-east striking cleavage dipping to the north-west, with more pronounced cleavage development in shale and phyllite (Oldow et al., 1984; Wyld, 2002). In the Humboldt range, a Jurassic pluton (age 165 Ma) intruded into Lower Jurassic rocks that contained deformation like that exhibited throughout the rest of the region (Wyld, 2002). Therefore, deformation occurred in Jurassic time prior to 165 Ma. However, on the scale of a large basin, the deformation may have been heterogeneous in space and time.

Closure of the Star Peak/ Luning basin in a back-arc setting produced contractional deformation and a fold and thrust belt, which developed in response to active convergence and eastward subduction along the continental margin. Deformation and magmatism moved progressively eastward as the continental margin continued to experience east-directed contraction. Phases of progressive eastward migration of deformation have been given different names (here listed from west to east): Luning-Fencemaker belt, Eureka belt, and the Sevier belt (Burchfiel et al., 1992).

Luning-Fencemaker Thrust Belt

The Luning-Fencemaker belt of deformation and magmatism is the earliest and western most of the three sets of thrust belts and was directly responsible for the closure of the Star Peak/Luning basin (Burchfiel et al., 1992). Magmatism during this period of deformation has been recognized in the Jackson Mountains and East Range of the north central Nevada. Plutons with ages of approximately 160 Ma as well as sills from another event, which yielded ages of 115 Ma, have been described in the Jackson Mountains (Maher and Saleeby, 1988). Within the East Range, a pluton was dated at between 160 Ma and 150 Ma using K/Ar from hornblende (Speed et al., 1988).

Deformation may have started in early Middle Jurassic, and thrusting clearly began by the late Middle Jurassic (Burchfiel et al., 1992). However, the detailed timing of the faulting and deformational events is poorly constrained. Thrusting and deformation related to the Luning-Fencemaker system played an important role in the history of the western United States because it represents the onset of compressional tectonism that lasted throughout the Cretaceous in the back-arc region of the Klamath and Northern Sierra arc (Burchfiel et al., 1992).

Eureka Thrust Belt

The Eureka belt of east central Nevada consists of continental deposits that formed in an active fold and thrust belt (Schmitt, 1989). Fold vergence appears to be toward the east; however, Bartley (1990) described thrust faults with both westward and eastward vergence. The age of deformation remains ambiguous; however, it has been interpreted to be Cretaceous (Aptian to Maastrichtian) based on the age of syn-

deformational deposits (Burchfiel et al., 1992). Shortening within the Eureka belt appears to be less than in the Luning-Fencemaker belt or the Sevier belt (Burchfiel et al., 1992).

Sevier Thrust Belt

The largest of the three deformational zones is the Sevier belt, which stretches from southern California into northern Canada (Burchfiel et al., 1992). The Sevier belt is characterized by eastward vergent folding and thrusting. Thrusting occurred after Jurassic plutonism at 165 and 150 Ma and prior to or synchronously with Late Cretaceous clastic wedge formation along the eastern margin of the uplift (Burchfiel et al., 1992). Flexural down warping along the eastern extent of the Sevier belt was likely caused by the loading of the thrust sheet to the west (Burchfiel et al., 1992). The down warping created a basin able to accommodate the sediment input from the uplifted thrust, which formed the clastic wedges.

ROCK UNIT DESCRIPTIONS

The purpose of this section is to review characteristics of many of the important formations exposed in the north-central East Range, with particular focus on the Upper and Lower Inskip Formation. General relationships between the units will be discussed here (see Plate 1), whereas structural relationships and tectono-stratigraphic correlation will be described later in the text.

Valmy Formation

In the East Range, the Valmy Formation has been mapped with three different subdivisions: a lower greenstone unit, a chert and argillite unit, and a quartzite unit (Whitebread, 1994). Each unit is interpreted to be bound by thrust faults. However, age constraints don't require any faults at all, or the contacts could be faulted with minor displacement (Ketner et al., 2000). The greenstone unit is lowest and consists of metamorphosed basalt. Above this is the chert argillite unit, which contains mostly chert and argillite but also contains some greenstone. The chert tends to have a characteristic pale green color that is not recognized in chert from other formations in the area. The uppermost Valmy Formation is a quartzite that has a distinctive dark grey color. It is vitreous and derived from fine to medium grained sand. White quartz veins that cut through the quartzite are common.

Lower Inskip Formation

The Lower Inskip Formation consists of arkosic sandstone, conglomerate, phyllite, siliceous argillite, quartzite, minor shale and limestone, and rare greenstone. Arkosic sandstones contain relatively large amounts of feldspar and biotite mica mixed with the dominantly sand-sized grains of quartz. It may be in part derived from volcaniclastic input. The presence of detrital mica in the Inskip Formation suggests a source rock of granitic composition for some of the clastic input (Ferguson et al., 1951). Conglomerates consist of pebble to cobble-sized clasts of quartzite with some lithic fragments and monomineralic pebbles of quartz and feldspar. Some large feldspar clasts up to approximately 1 centimeter in diameter have been found in pebble conglomerates throughout the section. In the lower half of the Lower Inskip Formation, large rounded cobble-sized clasts of quartzite similar to the Valmy Formation quartzite are present locally; however, other formations including the Vinini Formation and the Eureka Formation quartzite are also very similar. Therefore, during deposition the Lower Inskip Formation may have been relatively near a source of Valmy Formation quartzite. Phyllites are interpreted to have originated as hemipelagic sediment. Metamorphism has produced fine-grained secondary mica in the phyllite. A significant amount of the section may be phyllite because the rock type does not outcrop well and is commonly covered. Quartzite is located near the base of the Lower Inskip Formation and sporadically throughout the section. The quartzites of the Lower Inskip Formation are lighter in color, not vitreous, and do not have the white quartz veins that are characteristic of the Valmy Formation quartzites. In the Lower Inskip Formation, the quartzite is not as massive and

has penetrative foliation, whereas the Valmy Formation is massive and contains no visible foliation.

Minor amounts of shale and limestone are interbedded with the more common volcaniclastic sandstones, conglomerates, and phyllites. Shales tend to be thin bedded and fissile; they typically weather more easily and do not outcrop well. Shales can be found in outcrops where they are sandwiched between more competent rock types, which also retard the physical weathering of the shale. Limestone is also found in the Lower Inskip Formation, where it does not form prominent ledges or outcrop. Colluvium covers much of the limestone, causing it to appear discontinuous. Greenstone is absent in the lower part of the Lower Inskip Formation, and occurs sparsely in the upper half of the Lower Inskip Formation. Alteration in the greenstone is variable, ranging from highly altered, dark green, chlorite-rich rocks, to slightly altered basalt. Tuff layers occur sporadically in the lowest part of the unit, interbedded with the quartzites just above the contact with the Valmy Formation.

Upper Inskip Formation

Upper Inskip Formation rocks consist chiefly of amphibolite/greenstone, phyllite, and quartzite, with lesser amounts of limestone, volcanic, and volcaniclastic rocks. The protoliths of the amphibolites of the Upper Inskip Formation can be interpreted either as mafic volcanic flows or sills. Some of the amphibolites have hornblende crystals up to 13 mm in length with Garbenschiefer texture. Phyllites in the Upper Inskip Formation weather more easily than the surrounding rock and tend to not outcrop well. Unlike the

Lower Inskip Formation, the Upper Inskip Formation tends to have quartzite that is pervasive throughout the entire section, and contains less feldspar rich rocks.

Limestone in the Upper Inskip Formation displays characteristic weathering patterns, and outcrops usually have rounded edges with bulbous surfaces. The limestones have been interpreted as discontinuous (Hargett, 2002) and may represent olistostromal deposition. However, limestones have some characteristics that suggest conformable deposition, including conformity with bedding above and below the limestones, as well as lateral continuity of up to a kilometer along strike. Limestone typically appears to be silty micrite with very fine quartz grains.

Many of the layers throughout the Upper Inskip Formation have a tuffaceous appearance that may reflect a component of volcanic material. Tuffs are also present in the Upper Inskip Formation and are recognizable by their fine grained texture and white color. Many of the tuffs and volcaniclastic deposits range from 15-25 cm in bedding thickness, very few deposits are thicker.

Havallah Sequence

The Havallah sequence consists of chert and argillite interbedded with turbidites derived from siliciclastic and volcaniclastic sediments as well as calcareous deposits (Bruekner and Snyder, 1985). Deposition of the Havallah sequence exposed in the East Range may have occurred in a part of the basin where the lithology differs somewhat from the more common lithostratigraphy found farther to the east. The Havallah sequence of the East Range consist of chert, siliceous argillite, limestone, arkosic sandstone,

greenstone, and conglomerate with clasts of what appear to be Valmy Formation quartzite (Ketner et al., 2000).

Koipato Group

The Koipato Group, generally considered Triassic in age, is composed of the three different members (from bottom to top): the Limerick Member, the Rochester Member, and the Weaver Member. The Limerick Member contains andesite overlain by meta-sediments, and has not previously been recognized in the East Range. Stratigraphically above the Limerick Member is the Rochester Member, which consists of rhyolite, tuffs, and clastic rocks (Vikre, 1977). In the East Range, although still dominated by rhyolite, the Rochester Member contains more diverse clastic rocks, including siltstone, quartzite, and conglomerate. Above the Rochester Member lies the Weaver Member, which contains mostly rhyolite and volcaniclastic rocks (Vikre, 1977). The Weaver Member is not present in the north-central East Range.

Igneous Rocks

The Upper and Lower Inskip Formation contain two phases of intrusive magmatism. The first is Triassic in age and produced porphyritic granodiorite sills with K-feldspar phenocrysts 1-2 cm in length. These sills are contained solely in the Lower Inskip Formation and are not present in the Upper Inskip Formation. Similar porphyritic sills/dikes can be found in the Valmy Formation to the east and Havallah sequence to the north in Rockhill Canyon. It is noted that there are very few Triassic intrusions, and that they are volumetrically minor in north-central Nevada (du Bray, 2007). These intrusions

are located mostly in the Humboldt Range, but also occur in the East Range and the Stillwater Range as well and consist mainly of leucogranite plutons and Rhyolite porphyry dikes (Johnson, 1977). However, the research on Triassic plutonism in Nevada has been almost extensively done in the Humboldt Range with little work done elsewhere (Johnson, 1977).

The second phase of magmatism is Jurassic in age and is represented by plutons ranging in composition from granite to quartz-diorite. Jurassic sills and dikes are present in all formations of the north-central East Range. Jurassic plutonism in northern Nevada ranges in age from approximately 145 Ma to 175 Ma, with the majority of intrusive activity occurring between 155-160 Ma (du Bray, 2007). The formation of the Jurassic sills has been interpreted to have resulted from the “slab-window magmatism” created in a back-arc setting, which is related to the breakoff of the Mezcalera plate (du Bray, 2007).

REVIEW OF PREVIOUS WORK

The geology of the East Range and north-central Nevada has been studied by a number of previous workers. As context for the current study, the history of observations, nomenclature, and interpretation are reviewed below.

Ferguson et al., 1951

The Inskip Formation only occurs in the East Range, and was described originally by Ferguson et al., (1951). The lithology of the Inskip Formation was regarded as similar to that of the Harmony Formation as well as the Edna Mountain Formation. Ferguson et al. (1951) interpreted the Inskip Formation and Edna Mountain to be of Permian age and the Harmony Formation to be older than the Inskip Formation, but not older than Mississippian. Detrital mica in the Inskip Formation sediments could have been eroded from the Harmony Formation and then redeposited, or it could have had a primary granitic source. The contact on the north margin of the Inskip Formation with the Koipato Group was considered to be an angular unconformity due to the strong deformation and folding in the Inskip Formation and the lack of similar deformation in the Koipato Group (Ferguson et al., 1951). This relationship would have required relatively rapid deformation, uplift, and erosion to juxtapose the Koipato Group and Inskip Formation because both units were thought to be deposited during the Permian (Ferguson et al., 1951).

All Paleozoic and Triassic rocks in the East Range have been faulted and folded. Deformation and faulting occurred in several phases, starting in the late Paleozoic and continuing until the Jurassic (Ferguson et al., 1951). Thrust faulting and regional E-W contraction predominated during the late Paleozoic to Jurassic, and normal faulting and regional extension occurred during Tertiary time (Ferguson et al., 1951). The Jurassic intrusive rocks appear to not distort the folding of the Paleozoic rocks and cross-cut structural features (Ferguson et al., 1951). Older fault zones may have acted as conduits for the magma emplacement of the Jurassic igneous rocks (Ferguson et al., 1951).

Map relationships in the East Range by Ferguson et al. (1951) show the Inskip Formation on the western side of the East Range in depositional contact above the Leach (later called Valmy) Formation. The Inskip Formation was considered Permian in age and the Leach Formation was considered Carboniferous. These two formations were mapped as the hanging wall of a thrust, placing them structurally over rocks interpreted to be Triassic in age. Footwall rocks are exposed in a window cored with a Jurassic pluton near Lee Peak. New fossil age data from footwall rocks suggest an Ordovician age, and this unit may represent the Preble Formation (Whitebread, 1994; Ketner, 2008). To the north, the Inskip Formation and Leach Formation units are in contact with the Koipato Group. The relationship of the Leach Formation and Inskip Formation to the Koipato Group, however, was uncertain. In some places, the Inskip Formation and Leach Formation were interpreted to have been thrust over the Koipato Group, and in other places the contact between the Inskip Formation and Koipato Group appeared to be depositional.

Roberts et al., 1958

Observations about the geology in the north-central part of Nevada were made by Roberts et al. (1958) and provide an overview of a large area that included the East Range, and reinterpreted some aspects of the regional geology. Paleozoic rocks of Nevada were divided into an “eastern” and a “western” assemblage. The eastern assemblage consisted of autochthonous shelf deposits (typically limestone), and the western assemblage was interpreted as allochthonous, containing mainly clastic rocks, with up to 30% volcanic or volcaniclastic components (Roberts et al., 1958). The quartzites of the western clastic assemblage are generally more mature and clean but some sandstones contain lithic fragments and feldspar, suggesting immaturity (Roberts et al., 1958).

The Valmy Formation was assigned an age of Early to Middle Ordovician based on graptolite fauna (Roberts et al., 1958). Other quartzites in north-central Nevada are also of Ordovician age, including the Vinini Formation and the Eureka Formation, which also have similar composition to the Valmy Formation and may have derived from the same source (Roberts et al., 1958). The Vinini Formation has finer grain size than the Valmy Formation and may have been deposited farther from the source. Other Ordovician rock units contain no quartzite and were considered distal to the source of quartz (Roberts et al., 1958).

In late Devonian to Early Mississippian time, thrusting of the allochthonous western assemblage over the eastern assemblage caused folding of the eastern rocks and brought rock of similar age but different facies into structural contact (Roberts et al.,

1958). The new Antler highlands formed by this orogenic event provided a source for clastic input shed into adjacent basins. These new deposits were interpreted as the "overlap assemblage," with clastics being transported to the west and the east from the highlands (Roberts et al., 1958). Carbonate deposition continued on the eastern margin of the foreland basin, where the clastic influx was minimal. Clastic deposits shed to the west into the Havallah basin were likely about 50 to 100 miles from the Antler highlands, but now are located in the Sonoma and East ranges due to E-directed thrust transport in what Roberts et al. (1958) called the Mesozoic orogeny. Overprinting by these later orogenic events and different source rocks for the overlap sequence make correlation of the different rocks within the overlap sequence difficult (Roberts et al., 1958).

Different from the overlap assemblage but still upper Paleozoic in age are several formations that were interpreted by Roberts et al. (1958) to have been emplaced from a great distance. These units include the Inskip Formation, Havallah sequence, Koipato Group, and the Leach Formation (which was reinterpreted later as the Valmy Formation). The timing of thrusting that emplaced these formations was considered to be Mesozoic (Roberts et al., 1958). In the central East Range, the Inskip Formation and the Leach Formation were considered to be juxtaposed by faulting with the Inskip Formation structurally above the Leach Formation (Roberts et al., 1958). Because of similarities between the Valmy Formation and Leach Formation, Roberts et al. (1958) suggested that they may be equivalent. Due to lack of fossils in the Leach Formation, the age of the formation was poorly known, and interpreted to be Mississippian or older (Roberts et al., 1958). The age of the Inskip Formation was interpreted to be Mississippian from a poorly

preserved coral found in a shaly limestone in the lower half of the formation (Roberts et al., 1958).

The northern margin of the Inskip Formation in the East Range is in contact with the Koipato Group. This contact was interpreted by Roberts et al. (1958) to be a thrust. Apparently, the Inskip Formation and Leach Formation were thrust over the Koipato Group in this interpretation. Prior to this work, the Koipato Group was considered to be Permian in age based on the occurrence of Helicoprion in at least one locality. However, new fossil ammonites from other parts of the Koipato Group yielded ages of Early Triassic: Roberts et al. (1958) suggested that the Koipato Group may span from the Permian through the Early Triassic.

Silberling and Roberts, 1962

Silberling and Roberts (1962) provided additional data and interpretations of Paleozoic and Mesozoic formations in north-central Nevada. Their mapping of the central East Range still retained the names of Inskip Formation for the western formation and the Leach Formation for the eastern unit. The contact between the two formations was considered to be steeply faulted, with the Inskip Formation as the younger of the two formations (Silberling and Roberts, 1962). Age constraints remained poor. No fossil ages were identified for the Leach Formation, and it was assumed to be older than the Mississippian Inskip Formation. Therefore, the Leach Formation was constrained to Mississippian or older (Silberling and Roberts, 1962). A thin slice of the Havallah sequence just north of the Inskip Formation in the East Range produced Fusulinids that yielded an age of early Middle or late Early Permian (Silberling and Roberts, 1962).

The contact between the Inskip Formation and the Koipato Group was reinterpreted as a thrust, with the Inskip Formation in the hanging wall over the Koipato Group (Silberling and Roberts, 1962). This interpretation contrasted significantly with previous ideas that viewed the relationship as either depositional or the result of minor faulting. This structure was called the Willow Creek Thrust, and was thought to have been west-directed (Silberling and Roberts, 1962). This reinterpretation was necessary because the interpreted age of Mississippian for the Inskip Formation resulted in an older on younger relationship, while in previous work both formations were considered Permian in age and a depositional contact was likely. A key insight is that the formation underlying the Koipato Group in all cases is the Havallah sequence and not the Inskip Formation or Leach Formation as previously thought (Silberling and Roberts, 1962).

Other notable reinterpretations of the geology of the East Range made by Silberling and Roberts (1962) are as follows. The Leach Formation was given an age of Ordovician, perhaps due to correlation with the Valmy Formation. In the Rockhill Canyon area and stratigraphically below the Koipato Group, a thin slice of what had previously been interpreted as Inskip Formation was reinterpreted as Havallah sequence. The thrust between the Inskip Formation and the Koipato Group and the thrust separating the Leach Formation and Triassic units in the center of the domal structure were interpreted to be the same thrust and given a name of Willow Creek Thrust. There was still no age constraint on the metasedimentary rocks at the center of the domal structure and they continued to be of assumed Triassic age.

Johnson, 1977

Maureen Johnson (1977) finalized the correlation between the Leach and Valmy formations. The use of the term “Leach Formation” was dropped in the East Range and the distinctive massive dark grey vitreous quartzites were correlated with the Valmy Formation, which had been previously dated as Ordovician. Although the finer grained rock types within the Valmy Formation were not distinct enough to separate the unit from other Paleozoic units in the area, the quartzite was similar enough to correlate with the Valmy Formation in other areas (Johnson, 1977).

The Inskip Formation was divided into the lower and upper units based on mapping done by Donald Whitebread (1978), which was unpublished at the time. The relationship between the Valmy Formation (previously called Leach Formation) and the Inskip Formation still had not been resolved. The Valmy Formation and Inskip Formation were both believed to have overridden the Koipato Group to the north and the Triassic metasediments near Lee Peak along the Willow Creek Thrust. The thrust was interpreted to be of post Triassic age (Johnson, 1977). The Mississippian age given to the Inskip Formation may have been part of the basis for interpreting the Inskip Formation as part of the overlap sequence following the Antler orogeny (Roberts et al., 1958; Johnson, 1977).

Mapping shows the contact between the Valmy Formation and the Inskip Formation approximately where it is identified today, although the Upper and Lower Inskip Formation are not differentiated on the map. Mapped relationships in the Valmy Formation showed a thrust fault that separates the vitreous quartzite member and the finer grained chert, argillite, and greenstone member, with the quartzite member thrust over the finer grained member.

Whitebread, 1978

Donald Whitebread published his map in 1978 under the USGS open file report 78-407. The map was black and white with greater detail of the area than had been previously published. Separation of the Upper and Lower Inskip Formation was included in the mapping along with unit descriptions. Ages for the Upper and Lower Inskip Formation were assigned to Mississippian or Devonian or both. Whitebread (1978) used question marks next to the age of the Inskip Formation to highlight the fact that conclusive fossil ages had not yet been obtained; the coral from the Inskip Formation was given a likely Mississippian designation but significant uncertainty existed. Another interesting conclusion from Whitebread's (1978) preliminary map was the reinterpretation of the Triassic units in the center of the domal structure. A new fossil location is shown along the edge of the previously mapped Triassic unit. Although this fossil is not described or given an age, the interpretation of the units to potentially be Paleozoic in age gives insight into what he had found. The units are listed as either Mesozoic or Paleozoic in the correlation of units and in the description called "metasedimentary rocks of undetermined age" in the rock description section of the map (Whitebread, 1978).

The dome feature near Lee Peak, which exposed the meta-sedimentary rocks of undetermined age, was considered to be cored by a Jurassic pluton. Another pluton near the northern boundary of the Inskip Formation just south of Rockhill Canyon was also considered Jurassic. This pluton cross-cuts both the Upper and Lower Inskip Formation contact and the Lower Inskip Formation and the Valmy Formation contact. These two contacts were mapped as depositional. Cross-cutting relationships of the Jurassic pluton

show that the formations were in contact before the intrusion and are older than Jurassic in age. Another Jurassic pluton was mapped on the north side of Inskip Canyon. This pluton cross-cuts the Upper and Lower Inskip Formation contact and ends at the Inskip Formation-Valmy Formation contact. Unfortunately, none of the plutons in the area were radiometrically dated, and they were assigned ages based on their relationships with surrounding formations and correlation with dated plutons regionally.

North of the Willow Creek Thrust, the Havallah sequence was mapped in greater detail and divided into a couple of blocks separated by faults. Several Havallah sequence fossil locations are labeled and yielded fossils of Pennsylvanian and Permian age. Stratigraphically on top of the Havallah sequence above what was interpreted to be an angular unconformity lays the Rochester Member Rhyolite of the Koipato Group.

Elison, 1987

Like the interpretation of Silberling and Roberts (1962), the work of Elison (1987) concluded that the Willow Creek Thrust was a west vergent fault that brought Lower to Upper Paleozoic rocks from the east over Triassic rocks considered to be autochthonous and of a depositional shelf setting. The Willow Creek Thrust was interpreted to be a post-Fencemaker thrust, younger than late Middle Jurassic in age (Elison, 1987). Deformation was considered a result of the foreland fold and thrust belt of the Lunning-Fencemaker thrust system that developed in the Triassic rocks (Elison, 1987). However, because the Willow Creek Thrust occurred after the Fencemaker thrusting in this interpretation, the timing is problematic.

Elison (1987) focused mainly on the Triassic units in the northern part of the East range, and included little discussion of the Inskip and Valmy formations. He cited the complex nature of deformation in the Paleozoic rocks as a reason to not fully characterize the deformation in the area. However, he gave descriptions of the rocks and offered some interpretations, including the idea that the Harmony Formation of the far eastern East Range and the Valmy Formation may have been emplaced with the Roberts Mountains allochthon during the Antler orogeny and the Inskip Formation was formed in a basin to the west of the new highlands (Elison, 1987). Because the Inskip Formation contains clasts that look similar to the Valmy Formation quartzite, detritus from the Valmy Formation and the Harmony Formation may have been source rocks for filling the basin (Elison, 1987). An alternative theory is that the Harmony Formation and Valmy Formation were incorporated into an accretionary wedge that shed sediment westward, filling a forearc basin in which the Inskip Formation was deposited (Elison, 1987). The relationship of the Inskip Formation to the Roberts Mountains allochthon was "questionable," however (Elison, 1987).

Speed et al., 1988

The pluton at the center of the domal structure near Lee Peak in the East Range was dated at 151 Ma by biotite and hornblende using K-Ar geochronology (Speed et al., 1988). Typical uncertainties for K-Ar geochronology are about 3%. The K-Ar ages are cooling ages, so they may be minimum ages for magmatic crystallization. West-directed movement of the Willow Creek Thrust was interpreted to predate the emplacement of the pluton because of the lack of deformation exhibited in the pluton (Speed et al., 1988).

However, the timing of the Willow Creek Thrust was not well constrained. Triassic units north of the Paleozoic units of the overriding thrust have west vergent folding that may be related to the thrusting (Speed et al., 1988). One possible mechanism for the west-directed nature of the Willow Creek Thrust is intrusion of plutons along the Toiyabe uplift to the east of the East Range (Speed et al., 1988).

Whitebread, 1994

Adapted from his earlier map published in 1978, Whitebread (1994) published his geologic map of the Dun Glen Quadrangle in Pershing County, Nevada, which includes the northern half of the East Range at a scale of 1:48,000. Although contacts of unit boundaries were not changed, additions to the map include more recognizable fossil locations and their interpreted ages along with the geologist who identified them.

Although alluded to in his earlier map (Whitebread, 1978), the metasediments of the domal structure were formally assigned an age of Cambrian to Early Ordovician. This allowed for reinterpretation of the Willow Creek Fault around the dome. Whitebread (1994) indicated that the contact is faulted in some areas but need not be a thrust of great distance. It could be minor faulting with a low angle. The new interpretation did not require the presence a fault.

Ketner, 1998

Ketner (1998) reported that the East Range had not undergone a major folding event from the Middle Ordovician through the Middle Mississippian. Folding resumed during post Triassic time in the East Range, with folding of both the Paleozoic and

Triassic units. The folding caused similar deformation in both rock series (Ketner, 1998). Bedding of rocks near the contact between the Inskip Formation and the Valmy Formation shows concordance of strike and dip and was considered a disconformity (Ketner, 1998). Above the contact in the southern part of the East Range, the Inskip Formation has a basal conglomerate that has incorporated cobble-sized clasts of quartzite similar to the Valmy Formation quartzite (Ketner, 1998).

The fossil ages reported by Whitebread (1994) for the Valmy Formation argillite member were obtained from conodonts (Ketner, 1998). Reevaluation of the conodont fossils obtained from the Inskip Formation gave ages of early Late Mississippian, and the coral that gave the original age for the Inskip Formation was inferred to have been reworked. The conodonts may have been reworked as well (Ketner, 1998). Stratigraphically higher in the section, a conodont was found with an age of Morrowan, which is Early Pennsylvanian (Ketner, 1998). Due to the potential for the reworking of fossils, these ages were viewed as maximum ages for the formation.

The Havallah sequence just north of Rockhill Canyon on current maps was originally mapped by Ferguson et al. (1951) as part of the Inskip Formation. Ketner (1998) agreed with this interpretation and reassigned rock units. However, the mapped Willow Creek Thrust just south of Rockhill Canyon remained because the interpreted upper-most Inskip Formation was juxtaposed along strike with the lower-most Inskip Formation.

Ketner et al., 2000

Ketner et al. (2000) sought to reinterpret the map published by Whitebread (1994) by using new paleontological data to reevaluate interpretations of the unit contacts throughout the central East Range. In his view, after revision of ages, no need existed to call on large scale faulting from great distances because all the units followed the law of superposition with the oldest at the bottom and the youngest at the top. The name of Preble Formation (through correlation with similar units in other areas) was given to the unnamed metasedimentary rocks within the domal structure in the central East Range by Ketner et al. (2000). Preble Formation represents the oldest formation in the East Range, with an age of Cambrian to Early Ordovician, followed by the Valmy Formation, which is Ordovician (Ketner et al., 2000).

The Inskip Formation, Havallah sequence, and the Harmony Formation were all interpreted to be correlative based on the arkosic sandstones and conglomerates that exist in the lower part of the Havallah sequence, Inskip Formation, and the complete Harmony Formation. Although the Harmony Formation is generally considered Cambrian in age, Late Devonian ages have been reported for the Harmony Formation in the Hot Springs Range (Jones, 1997). In the East Range, the Harmony Formation has been assumed to be Devonian in age (Ketner et al., 2000). New fossil data for the Upper Inskip Formation yielded Permian Conodonts, which changed the Inskip Formation age from Late Devonian in the lower member to Permian in the upper (Ketner et al., 2000). Fossil constraints on the Havallah sequence give the unit an age of Mississippian through Permian (Ketner et al., 2000), which is remarkably similar to the Inskip Formation ages. Due to these similarities in rock types and ages, the three were interpreted as the same

lithostratigraphic unit within the East Range by Ketner et al. (2000). Above the Upper Paleozoic units, the Triassic Koipato Group appears to be in an angular unconformable relationship over the mapped Havallah sequence just north of Rockhill Canyon. All these units rest concordantly on the Valmy Formation, which lies on the Preble Formation, which was interpreted as an undisrupted sedimentary stack other than a time of non-deposition or erosion from Middle Ordovician through Late Devonian/Early Mississippian (Ketner et al., 2000).

Because the Willow Creek Thrust segment at the central area of the domal structure was no longer necessary, a reinterpretation of the thrust just south of Rockhill Canyon was also attempted. Rather than interpreting it to be a thrust, Ketner et al. (2000) called for a high-angle reverse fault of moderate magnitude to juxtapose the Havallah and the Inskip Formationin the Rockhill Canyon area. The domal structure is interpreted to have occurred when the Jurassic pluton was emplaced into the central East Range, distorting the stratigraphy.

Hargett, 2002

Reinterpretation of geology and placement of the Willow Creek Thrust was made by Hargett (2002) to follow the Valmy Formation and Inskip Formation contact. Evidence for the presence of a fault at this contact includes a west vergent drag fold in the Inskip Formation near the contact, a considerable increase in strain magnitude adjacent the contact, and horizontal fold axes, which are present in the Inskip Formation but not the Valmy Formation (Hargett, 2002). The thrust was interpreted to be linked possibly to the Clear Creek Thrust system or Golconda Thrust of the Sonoma Range

(Hargett, 2002). The age of thrusting the Inskip Formation over the Valmy Formation, and the age for the folding within the formations were considered post Triassic due to the over thrusting of Triassic units in the northern part of the East Range (Hargett, 2002).

Identification of conodonts from the Inskip Formation was done by Tamra Schiappa from Boise State University and given an Early Pennsylvanian age (Hargett, 2002). However, the fossil was collected from a limestone outcrop on the south side of Inskip Canyon that is within several meters of a limestone that contained conodonts of Early Mississippian age (Hargett, 2002), thereby raising the concern that some if not all of the fossils could be redeposited and only provide maximum age constrains on the Inskip Formation.

Structural analysis identified three phases of deformation: (1) penetrative foliation, (2) west vergent folding, and (3) localized deformation surrounding plutons, due to their emplacement.

Ketner, 2008

Two different phases of metamorphism were interpreted in the Inskip Formation, the first occurred when new igneous rocks came into contact with seawater, causing plagioclase to convert to albite and the mafic minerals to convert to hornblende (Ketner, 2008). The second phase of metamorphism was caused by heat and pressure, at the same time a shear stress that was parallel to bedding (Ketner, 2008) caused deformation, which formed the penetrative foliation that is characteristic of the Inskip Formation in all but the youngest dikes and sills that intruded after the metamorphism and deformation. Metamorphism was thought to be more intense in the older beds and less intense in the

younger beds (Ketner, 2008). Timing of the second stage of Metamorphism had not been resolved but the Triassic Rochester Member Rhyolite of the Koipato Group is clearly affected, indicating an age of post Triassic (Ketner, 2008).

Thicker, more competent beds appear to be less susceptible to deformation and dynamic recrystallization than the thinner beds, resulting in less deformation and shear induced thinning (Ketner, 2008). Fine grained felsic volcanic rocks termed “felsites” are common in the Upper Inskip Formation and are either sills that intruded after deposition of the formation or flows and/or very shallow intrusions that occurred concurrently with the deposition of the clastic rocks (Ketner, 2008). Some of the felsites do not exhibit any deformation and likely represent sills rather than flows.

FOCUS OF CURRENT WORK

There remain several items to be addressed that the focus of this study will try to reveal. The work will use geologic mapping, U-Pb geochronology, and structural analysis to determine the structural and deformational history of the Inskip Formation, and constrain the timing of major deformational episodes. Additionally, the depositional age of the Inskip Formation will be refined through U-Pb geochronology of volcanic deposits. Finally, the study will evaluate the regional significance of the Inskip Formation and its relationship within the surrounding tectono-stratigraphic framework.

RESULTS OF CURRENT STUDY

Structural Analysis and Interpretation

Observations

Nearly all rocks in the Upper and Lower Inskip Formation contain well-developed penetrative foliation (Figure 2) sub-parallel to original bedding (Figure 3). In some lithologies, the foliation appears to have formed primarily due to pressure solution (Figure 4). Poles to planes of this (D_3) foliation scatter in a subvertical, NW-SE striking girdle, consistent with SE-trending folding of later deformation (Figure 5). In general, the penetrative foliation strikes north/northeast and dips moderately to steeply to the northwest at an average dip of approximately 51.5 degrees. A stretching lineation lies within the plane of penetrative foliation and typically plunges to the west (Figure 6). The measurement plunging to the east was taken in Rockhill Canyon just north of the mapped segment of the Willow Creek Thrust as mapped by Whitebread (1978) and may have mineral alignment produced by later faulting. Two measurements that show a more northward plunge come from the eastern limb of folds, and are consistent with the lineation and foliation having formed prior to folding. When viewed on surfaces parallel to lineation and perpendicular to foliation, clasts within the conglomerate layers display sigma-type wings, which are useful as kinematic indicators. However, ambiguity exists in the direction of shear indicated by the winged clasts. Apparent kinematics vary from

outcrop to outcrop: some show a west-directed shear (Figure 7) while others indicate an east-directed shear.

Petrographic analysis of oriented thin sections (all sections were cut perpendicular to foliation and parallel to lineation) show other kinematic indicators, including sigma-style winged porphyroclasts, quarter structures, and tiled feldspar grains. The quarter structures (Figure 8) and the sigma porphyroclasts (Figure 9) yield consistent shear sense of top to the west. In the tiled feldspar grains (Figure 10, and 11), the direction of shear varies. This variability may reflect the original orientation of the feldspar grain before deformation and the way the grains rotated during deformation, particularly if the bulk deformation included a component of pure shear.

Folding of bedding/foliation is common in the north-central East Range. Folds generally show an east-directed vergence (Figure 12); however, a few exist with vergence to the west (Figure 13). Folds range from the scale of centimeters (Figure 14) to large folds that are tens of meters. Chevron-style folding (Figure 15) is documented in the upper-most part of the Valmy Formation. The study area is located in the NW limb of a large antiform that trends to the southwest. The east-verging folds could be parasitic to this larger structure (e.g., Hargett, 2002).

In the vicinity of the contact between the Valmy Formation and the Lower Inskip Formation, slicken lines are common in the quartzite of the Valmy Formation (Figure 16). Although the slicken lines have been folded, they are generally oriented in an east-west direction.

Crenulation cleavage (Figure 17) developed locally in mica-rich layers, such as shale and phyllite. Along the western flank of several folds, in the Inskip Formation,

crenulation cleavage also developed. Strike of the crenulation cleavage is generally to the northwest with the dip steeply to the southwest (Figure 18). This orientation is present in both the shale/phyllite layers and along the western limbs of the folds.

Other structural features observed include kink bands, c/s fabrics, folded quartz veins (Figure 19), boudinage of quartz veins (Figure 20), and rootless isoclinal fold hinges (Figure 21). The kink bands strike north-south and dip steeply. Quartz veins are present throughout the field area and are most distinguishable in the quartzites of the Valmy Formation. Depending on orientation, the veins were either folded by shortening or stretched to form boudins.

Figure 2. Field Photograph Showing Penetrative Foliation in an Amphibolite Layer. White Bar Represents Foliation Orientation. View is to the Northwest. Pen for Scale.

Figure 3. Field Photograph Showing the Orientation of the Penetrative Foliation (Solid Line), which Cuts Obliquely Across the Sharp Bedding Contact with Phyllite Below and Coarse Volcaniclastic Sandstone Above (Dashed Line). View to the Northwest, Coin for Scale.

Figure 4. An Example of Pressure Solution Cleavage in Quartzite of the Lower Inskip Formation. Note Quartz Vein Cut by Pressure Solution Seams Just to the Right of the Hammer Head. View to the North.

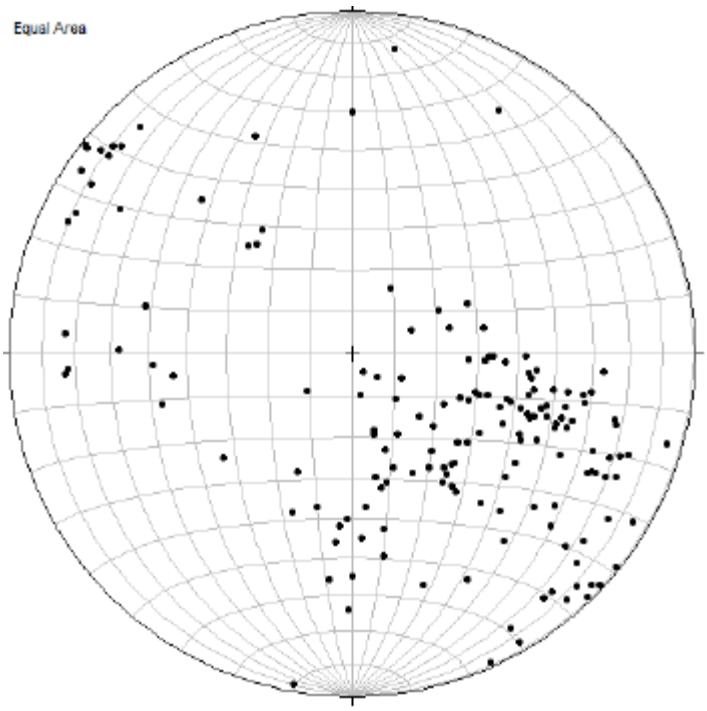

Figure 5. Stereo Plot of Poles to Planes of Penetrative Foliation.

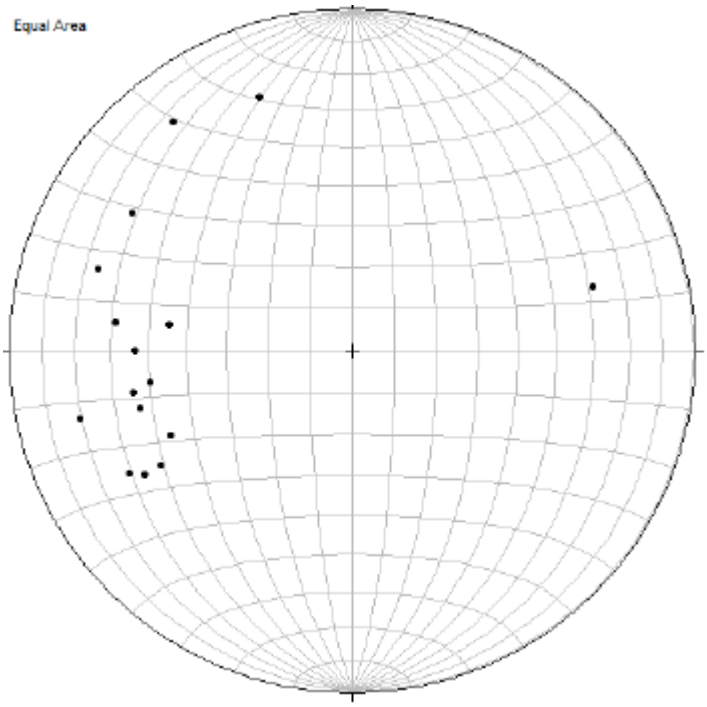

Figure 6. Stereo Plot of Stretching Lineation Contained Within the Penetrative Foliation.

Figure 7. View Looking North at an Outcrop Surface Perpendicular to Foliation and Parallel to Lineation. Sigma-Type Tails on cm-Scale Porphyroclasts Are Consistent with Sinistral (Top to the West Shear Sense) Tectonic Transport. Arrows Show Sense of Shear.

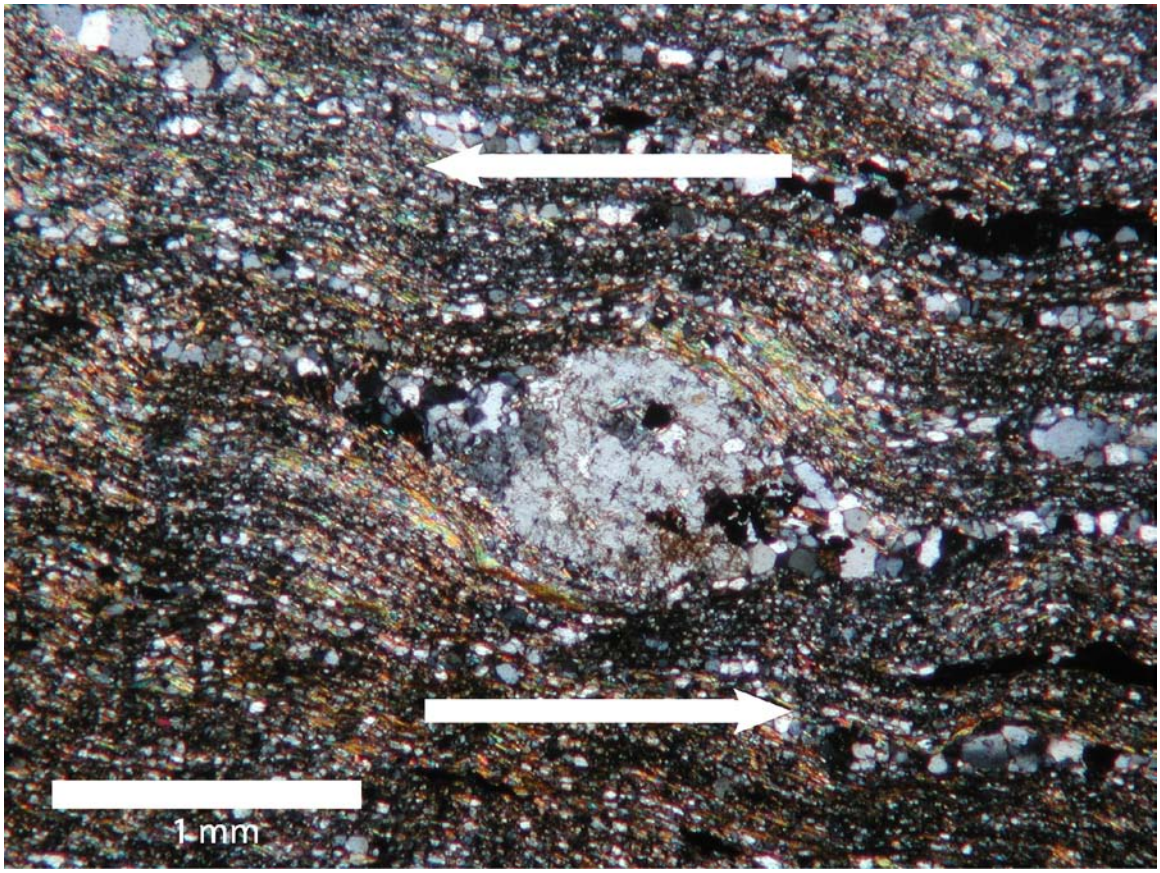

Figure 8. Photomicrograph of Sample 08JW534 Is Showing Quarter Structure Around a Feldspar Crystal, Consistent with Sinistral (Top to the West Shear Sense), View Looking North. Section Cut Parallel to Lineation and Perpendicular to Foliation.

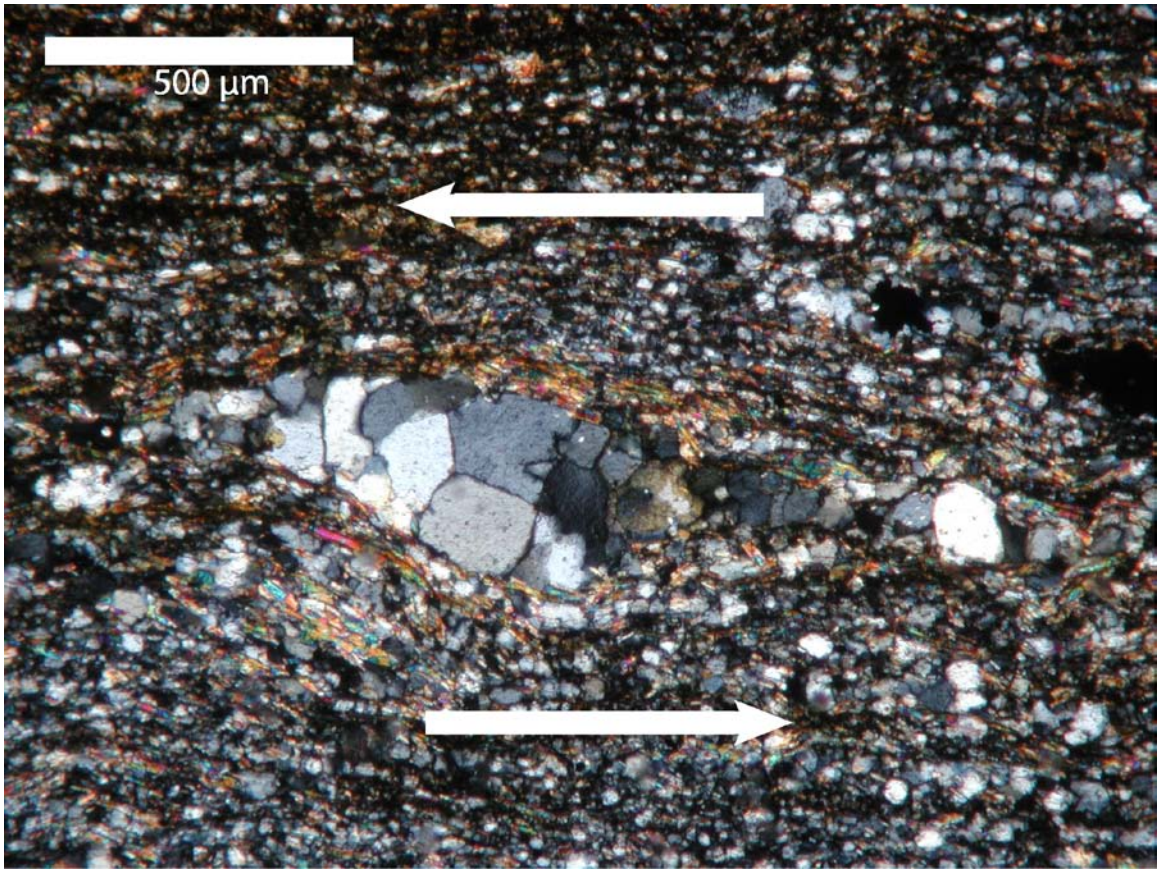

Figure 9. Photomicrograph of Sample 08JW534 Is Showing Sigma Porphyroclast Quartz Grain, Consistent with Sinistral (Top to the West Shear Sense), and View Looking North. Section Cut Parallel to Lineation and Perpendicular to Foliation.

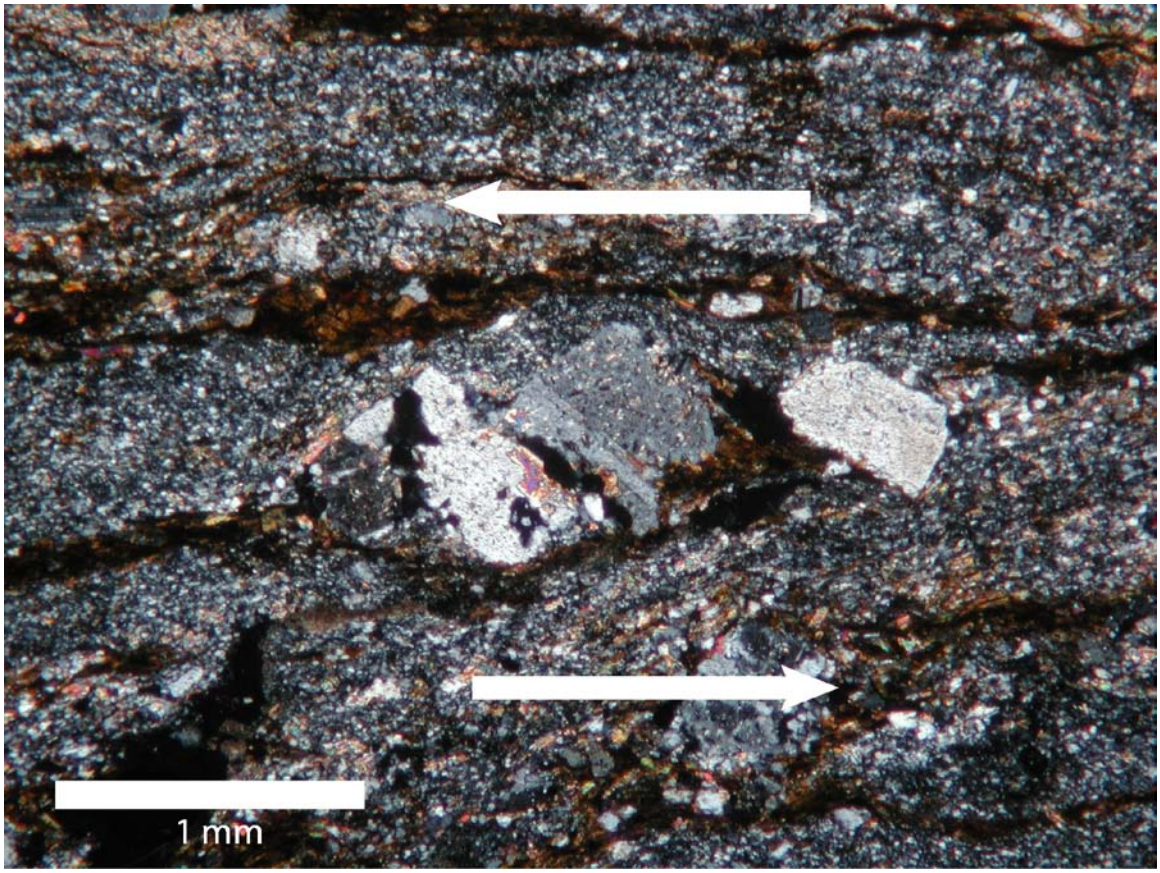

Figure 10. Photomicrograph of Sample 08JW691 Is Showing a Tiled Feldspar Crystal, Consistent with Sinistral (Top to the West Shear Sense), View Looking North. Section Cut Parallel to Lineation and Perpendicular to Foliation.

Figure 11. Tiled Feldspar Grains in Outcrop. Nickel for Scale, View to the South.

Figure 12. Field Photograph of East Verging Fold (View Looking North). Dashed Lines Represent the Trace of Folded Penetrative Foliation. Arrows Show Top to the East Shear Sense. Backpack for Scale.

Figure 13. West Verging Fold in Volcaniclastic Sandstone of the Lower Inskip Formation. Dashed Lines Represent the Trace of Folded Penetrative Foliation. Arrows Show Top to the West Shear Sense, View Looking to the North.

Figure 14. Field Photograph Showing Small Scale Folding or Parasitic Folds on the Larger Broad Fold in the Inskip Formation (View Looking to the North). There is also Nearly Vertical Crenulation (Axial Surface) Cleavage Related to Broad Fold of Original Foliation/Bedding.

Figure 15. Field Photograph Showing a Chevron Fold in the Valmy Formation Quartzite. View Looking to the North.

Figure 16. Field Photograph of Slickenlines Near the Valmy Formation and Lower Inskip Formation Contact. View Looking to the North.

Figure 17. Field Photo of Phyllite Layer with Penetrative Foliation Dipping Gently to Left (Solid Bar) and the Secondary Crenulation Cleavage Dipping Steeply to the Left (Dashed Line). View Looking NE.

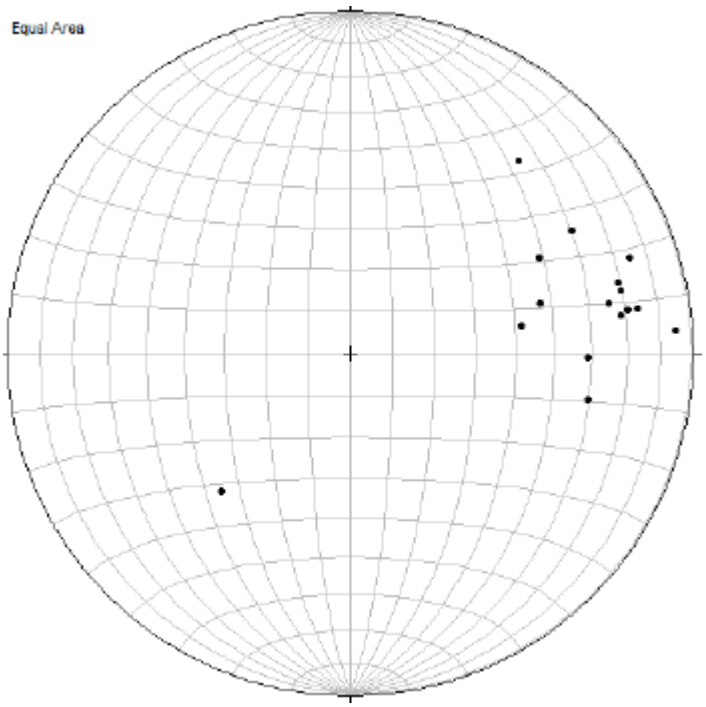

Figure 18. Poles to Planes of Crenulation Cleavage. Data Have a Tighter Grouping than the Poles to Folded Penetrative Foliation.

Figure 19. Field Photograph of Folded Quartz Vein in the Lower Inskip Formation. View to the South.

Figure 20. Field Photograph of Boudinaged Quartz Vein in the Lower Inskip Formation. Nickel for Scale, View to the North.

Figure 21. Rootless Isoclinal Fold Hinge with a Top to the East Sense of Shear. View Looking to the North. Coin for Scale.

Interpretation of Deformational History

At least five phases of deformation exist in the upper Paleozoic and early Mesozoic rocks of the East Range. These are recognized through structural interpretation and stratigraphic or plutonic cross-cutting relationships. The earliest phase of deformation (D_1) is recorded by the angular unconformity between the Upper/Lower Inskip Formation with the Rochester Member Rhyolite. Tilting and erosion occurred in older rocks prior to deposition of the Rochester Member. Timing of the deformation is bracketed by Early Triassic deposition of the Upper Inskip Formation (after 249.08 +/- .14 Ma (Sample 08JW534)) and the deposition of the Rochester Member Rhyolite, which has also been interpreted to be Early Triassic (fission-track age of 225 +/- 30 Ma, and Koipato Group isochron, which yields an age of approximately 235 Ma (Vikre, 1977)). Ammonites from the Star Peak Group, which overlies the Koipato Group, are interpreted to be Anisian in age (early Middle Triassic) (Silberling and Wallace, 1969; Geissman et al., 1990). Similar relationships occur regionally and have been attributed to the Sonoma orogeny (Silberling and Roberts, 1962). The Koipato Group overlies deformed upper Paleozoic rocks across an angular unconformity in many locations. Deformation in this phase could potentially have formed from block faulting or tilting in a caldera, in which case the implications for this phase to be related to the Sonoma orogeny is lessed.

The second phase of deformation (D_2) is the thrust emplacement of upper Paleozoic and lower Mesozoic basinal rocks, including the Lower and Upper Inskip Formation as well as the Rochester Member Rhyolite, over the lower Paleozoic rocks of the Valmy Formation. This thrust is correlated with the Golconda Thrust exposed in the south-central East Range, Sonoma Range, and Golconda Summit to the east of the study

area. The Golconda Thrust has been considered Late Permian to Early Triassic (Silberling and Roberts, 1962). However, cross-cutting relationship in the north-central East Range have the Golconda Thrust cutting the Rochester Member of the Koipato Group (Early Triassic), which establishes a Mesozoic age for the timing of the Golconda Thrust. This validates the speculation that the Koipato Group could have ridden the Golconda Thrust "piggyback" on the upper Paleozoic rocks during emplacement of the Golconda allochthon (Burchfiel et al., 1992). The Golconda Thrust is cross-cut by a late Middle Jurassic pluton (Sample 09JW891), which establishes a minimum age of thrusting (discussed in more detail below).

The third phase (D_3) resulted in the strong, synmetamorphic penetrative deformation that produced foliation, transposed original bedding, and a stretching or mineral alignment lineation. Kinematic indicators were observed and used to interpret direction of shear during the third phase of deformation. Micro structures obtained from oriented thin sections cut parallel to lineation and perpendicular to foliation were identified from both the Upper and Lower Inskip Formation. Samples from each unit exhibit a top to the west sense of shear. Small feldspar crystals from the felsic tuff collected in the Upper Inskip Formation exhibit quarter structures (Figure 8) and sigma type recrystallized tails (Figure 9), showing a top to the west sense of shear. Thin sections made from sample 08JW691 (a Triassic sill with feldspar phenocrysts up to 2.5 cm from the Lower Inskip Formation) also show quarter structures, sigma porphyroclasts, and tiled feldspar grains (Figure 10), each of which shows a west-directed sense of shear. However, due to the original orientation of some of the feldspar crystals, they may have back rotated in the strain field and give the appearance of an east sense of shear.

Consequently, tiled grains are less reliable indicators, and quarter structures and the sigma porphyroclasts were used to determine the bulk shear sense. Sigma-type winged quartzite cobbles in the Lower Inskip Formation show a west-directed sense of shear in some places (Figure 7), and east-directed shearing in other places. This variability may reflect a significant pure shear component of the bulk strain, rather than a consistant, unidirectional sense of tectonic movement during D_3.

Map scale folding trending from SW to NE is the fourth phase of deformation (D_4). In the East Range, this is exhibited by a large antiform that trends southwest to northeast and is cored by the Jurassic pluton near Lee Peak. To the east is a regional scale synform outlined by the trace of the Golconda Thrust as it closes around the Edna Mountain area (Figure 22). This series of folds appears to be west vergent as evidenced by the steep dip of the western limb of the antiform, which is locally vertical to overturned.

The fifth phase of deformation (D_5) resulted in the folding of the penetrative foliation and development of a crenulation cleavage (Figure 12). Most of the folds in the Upper and Lower Inskip Formation verge to the east/southeast, with antiforms having long shallowly dipping western limbs and short more steeply dipping eastern limbs. Poles to planes of the penetrative foliation scatter along a great circle, a pattern that can be attributed directly to the folding in this phase of deformation. The larger number of measurements on the more shallowly dipping limbs of the folds and areas that are folded less, versus the smaller number of steeply dipping eastern fold limbs also shows the east/southeast vergence in the folding. More specifically, the vergence is to the southeast with the average shortening direction to approximately 121 degrees (Figure 23) with a

fold hinge trend of 31 degrees and plunge of 5 degrees. The antiform (D_4) and the folds described as D_5 folds both formed by southeast-northwest contraction and therefore may be parasitic folds on the western limb of the anticline. In this case, the timing of the folding would be during the forth phase of deformation. The folding may be better described as D_{4-5} folds. Very few folds were documented with a top to the west vergence.

D_5 resulted in the local formation of a crenulation cleavage (Figure 17) in the less competent shale and phyllite of the Inskip Formation and along some of the western limbs of (D_{4-5}) folds. This crenulation cleavage may not be disconnected from the outcrop scale folding because cross-cutting relationships do not exclude the deformation from being synchronous. However, the fact that the crenulation cleavage reflects a relatively east-to-west shortening direction (in contrast to the folds) and the fact that crenulation cleavage orientations have not been folded after formation to the extent that penetrative foliation has seems to imply that the crenulations were formed at a later time (Figure 18). In addition to the crenulation cleavage, some D_{4-5} folds appear to have been refolded during a later phase, which would be included in this phase of deformation. Kink bands also have an orientation that is consistant with the shortening direction of this phase of deformation. The quartz grains in the relatively undeformed Jurassic sill exhibit undulose extinction, which may have been produced by latest stages of D_5 (Figure 24).

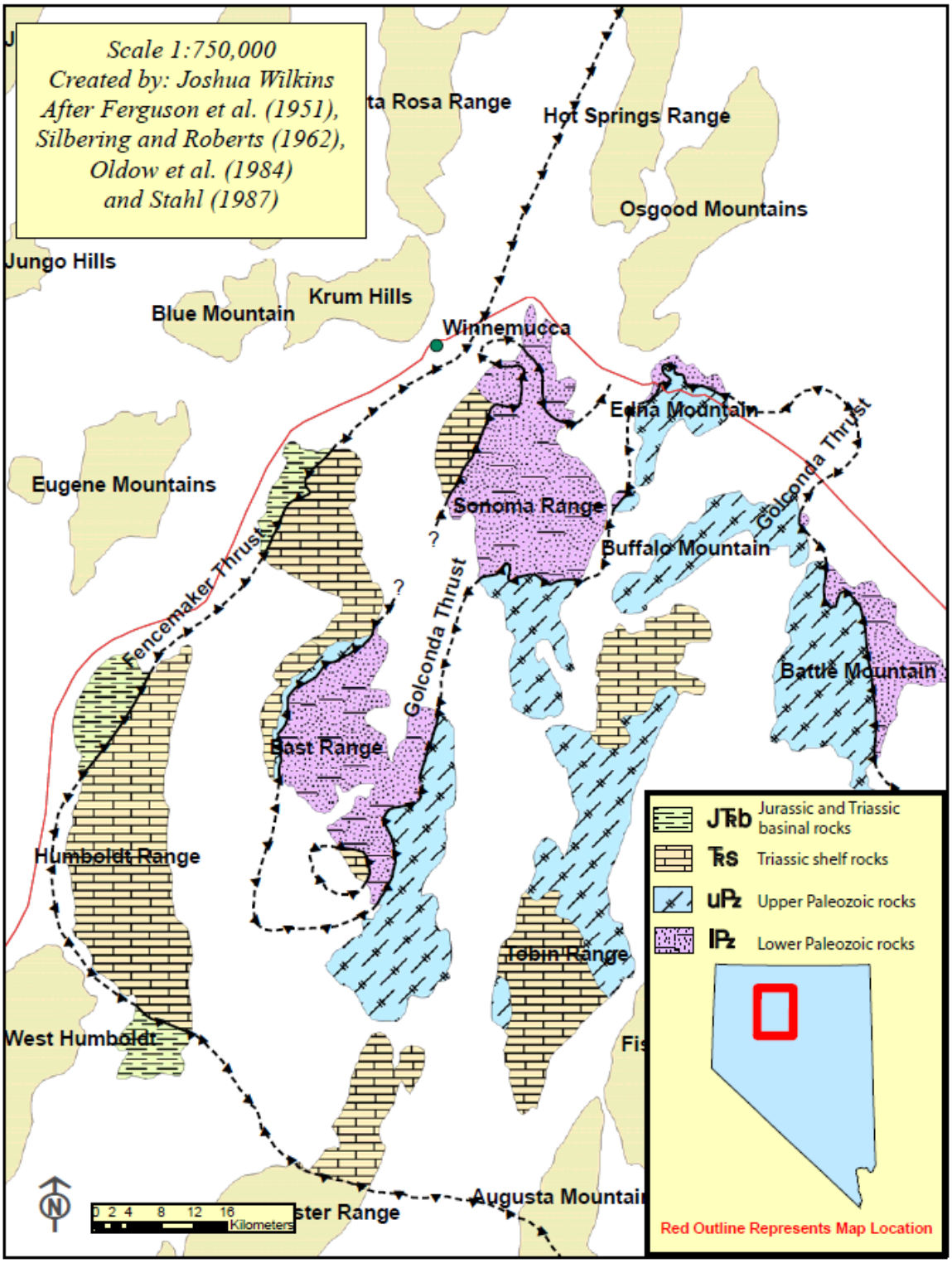

Figure 22. Simplified Geologic Map Showing Northeast Southwest Trending Antiform and Synform Outlined by the Trace of the Golconda Thrust.

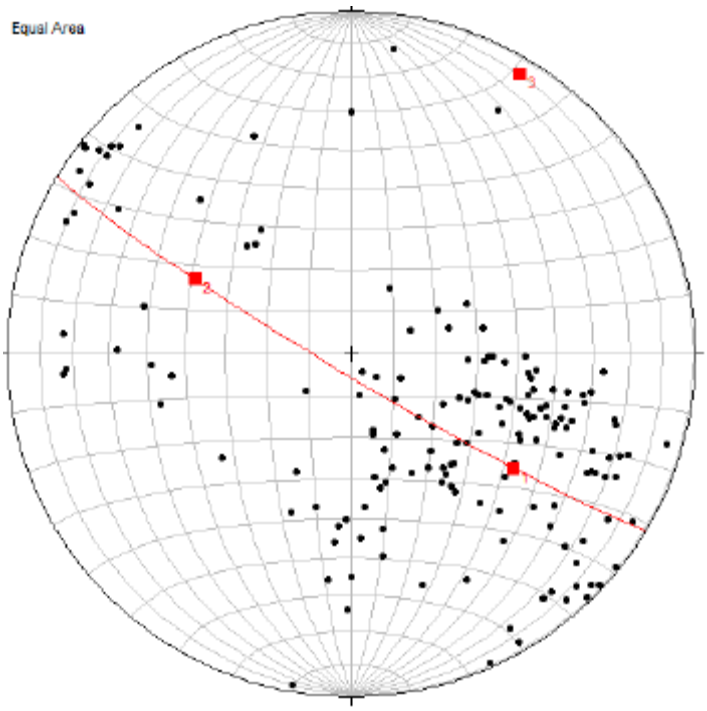

Figure 23: Stereo Plot Showing Analysis of $D_{4\text{-}5}$ Deformation Causing Scatter in D_3 Foliation Poles. Average Shortening Direction Implied for $D_{4\text{-}5}$ Folding Is Approximately 121 Degrees, with a Fold Hinge Trend of 31 Degrees and Plunge of 5 Degrees.

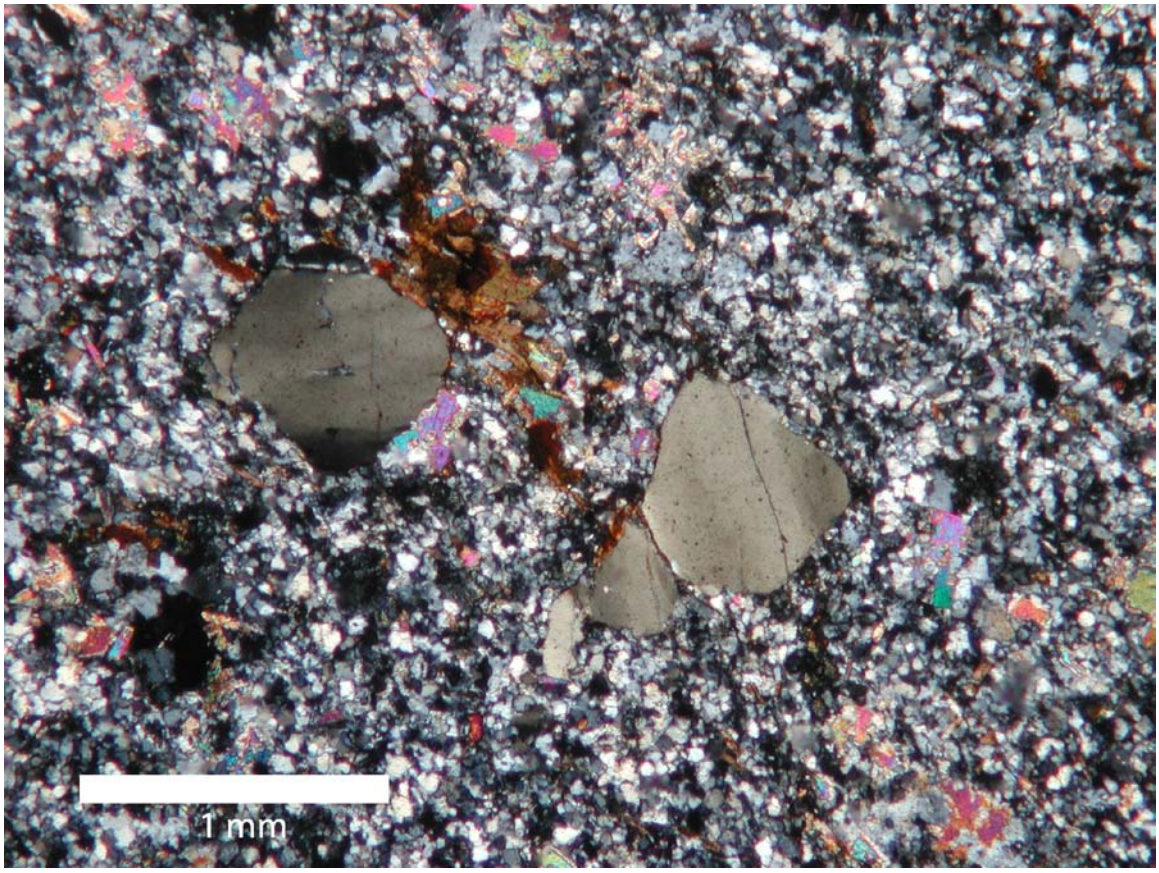

Figure 24. Photomicrograph of Sample 08JW661 Showing Undulose Extinction of Quartz Grains in Jurassic Sill.

Geochronology

Questions to be addressed through the application of geochronology include: (1) what is the depositional age of the Inskip Formation? and (2) what is the timing of deformation? Volcanic units within the Inskip Formation were sampled for U-Pb zircon geochronology to constrain the age of the sequence. In addition, sills and plutons, exhibiting cross-cutting relationships and/or having different amounts of deformation, were sampled to determine the timing of deformation.

U-Pb Geochronology Methods

Each sample consisted of approximately 10 Kg of rock extracted directly from outcrop. Heavy mineral separates were generated using standard techniques for crushing, magnetic separation, and heavy liquid separation.

Zircon was subjected to a modified version of the chemical abrasion method of Mattinson (2005), reflecting a preference to prepare and analyze carefully selected single crystals or crystal fragments. Zircon separates were placed in a muffle furnace at 900°C for 60 hours in quartz beakers. Single crystals were then transferred to 3 ml Teflon PFA beakers, rinsed twice with 3.5 M HNO_3, and loaded into 300 μl Teflon PFA microcapsules. Fifteen microcapsules were placed in a large-capacity Parr vessel, and the crystals partially dissolved in 120 μl of 29 M HF with a trace of 3.5 M HNO_3 for 10-12 hours at 180°C. The contents of each microcapsule were returned to 3 ml Teflon PFA beakers, the HF removed and the residual grains rinsed in ultrapure H_2O, immersed in 3.5

M HNO_3, ultrasonically cleaned for an hour, and fluxed on a hotplate at 80°C for an hour. The HNO_3 was removed and the grains were again rinsed in ultrapure H_2O or 3.5M HNO_3, before being reloaded into the same 300 µl Teflon PFA microcapsules (rinsed and fluxed in 6 M HCl during crystal sonication and washing) and spiked with the EARTHTIME mixed ^{233}U-^{235}U-^{205}Pb tracer solution (ET535). These chemically abraded grains were dissolved in Parr vessels in 120 µl of 29 M HF with a trace of 3.5 M HNO_3 at 220°C for 48 hours, dried to fluorides, and then re-dissolved in 6 M HCl at 180°C overnight. U and Pb were separated from the zircon matrix using an HCl-based anion-exchange chromatographic procedure (Krogh, 1973), eluted together and dried with 2 µl of 0.05 N H_3PO_4.

Pb and U were loaded on a single outgassed Re filament in 2 µl of a silica-gel/phosphoric acid mixture (Gerstenberger and Haase, 1997), and U and Pb isotopic measurements made on a GV Isoprobe-T multicollector thermal ionization mass spectrometer equipped with an ion-counting Daly detector. Pb isotopes were measured by peak-jumping all isotopes on the Daly detector for 100 to 150 cycles, and corrected for 0.22 ± 0.04%/a.m.u. mass fractionation. Transitory isobaric interferences due to high-molecular weight organics, particularly on ^{204}Pb and ^{207}Pb, disappeared within approximately 30 cycles, while ionization efficiency averaged 10^4 cps/pg of each Pb isotope. Linearity (to $\geq 1.4 \times 10^6$ cps) and the associated deadtime correction of the Daly detector were monitored by repeated analyses of NBS982, and have been constant since installation. Uranium was analyzed as UO_2^+ ions in static Faraday mode on 10^{11} ohm resistors for 150 to 200 cycles, and corrected for isobaric interference of $^{233}U^{18}O^{16}O$ on $^{235}U^{16}O^{16}O$ with an $^{18}O/^{16}O$ of 0.00205. Ionization efficiency averaged 20 mV/ng of each

U isotope. U mass fractionation was corrected using the known $^{233}U/^{235}U$ ratio of the ET535 tracer solution.

U-Pb dates and uncertainties were calculated using the algorithms of Schmitz and Schoene (2007), a $^{235}U/^{205}Pb$ ratio for ET535 of 100.18 ± 0.05, and the U decay constants recommended by Steiger and Jager (1977). $^{206}Pb/^{238}U$ ratios and dates were corrected for initial ^{230}Th disequilibrium using a Th/U[magma] of 3 ± 1 using the algorithms of Crowley et al. (2007), resulting in a systematic increase in the $^{206}Pb/^{238}U$ dates of ~90 kyrs. Common Pb in analyses up to 1 pg was attributed to laboratory blank and subtracted based on the measured laboratory Pb isotopic composition and associated uncertainty. This simple correction is typical of most analyses; occasional analyses with common Pb in excess of 1 pg were assumed to contain initial Pb within mineral inclusions, which was subtracted based on the model two-stage Pb isotope evolution of Stacey and Kramers (1975). U blanks are difficult to precisely measure, but are <0.1 pg. Over the course of the experiment, isotopic analyses of the TEMORA zircon standard yielded a weighted mean $^{206}Pb/^{238}U$ age of 417.43 ± 0.06 (n=11, MSWD = 0.8).

Results

Geochronologic data are reported in Table 1, and sample locations are shown on Figure 25. All ages reported are weighted mean dates at the 95% confidence interval. Location for each sample is reported in WGS 1984 datum, and UTM zone 11 N projection.

Age of Inskip Formation

Three samples were collected from different stratigraphic levels of the Inskip Formation. Two of these samples came from the Upper Inskip Formation (samples 08JW71, and 08JW534), and one came from the Lower Inskip Formation (sample 08JW131).

Sample 08JW71- Upper Inskip Formation

– UTM 0419616E, 4494890N

Sample 08JW71 is a fine grained tuffaceous phyllite in the upper portion of the exposed Upper Inskip Formation section.

Seven single-crystal fractions of zircon were analyzed from sample 08JW71 (Figure 26), z2 yielded a 206Pb/238U age of 248.80 +/- 0.22 Ma for the single grain. The other six grains yielded dates ranging from 114.07 +/- 0.08 Ma to 90.22 +/- 0.07 Ma, all of which are Cretaceous. Because the section from which this sample was collected contains dikes and sills of Jurassic age, this rock must be older than Jurassic, and the apparent Cretaceous ages must be related to neoblastic zircon growth. The sample could not have been deposited during the Cretaceous. This leaves the date obtained from z2, which alone does not provide a robust age; however, it is at least consistent with a depositional age of approximately 249 Ma. Given the wide dispersion of dates from individual grains and clear evidence of complex systematics, no age can be resolved for this sample with confidence.

Sample 08JW534- Upper Inskip Formation

– UTM 0420659E, 4494484N

Sample 08JW534 is a felsic tuff (Figure 27) within the lower half of the Upper Inskip Formation. The tuff is fine grained and contains feldspar phenocrysts. Petrographic analysis showed somewhat larger feldspar grains approximately 1-2.5 mm in size in a very fine grained matrix of mostly quartz with some feldspar and mica (Figure 8).

Nine zircon grains were analyzed from sample 08JW534 (Figure 28a-b). Six zircon yielded 206Pb/238U dates with a weighted mean date of 249.08 +/- 0.14 Ma (MSWD=3.3), interpreted as the depositional age of this tuff. Three grains are slightly younger (between 248.22 Ma and 244.69 Ma) and are interpreted to have younger metamorphic rims, similar to the neoblastic zircon of sample 08JW71.

Sample 08JW131- Lower Inskip Formation

– UTM 0423781E, 4495031N

Sample 08JW131 was collected near the base of the Lower Inskip Formation and is interpreted to be a tuff (Figure 29). The tuff is very fine grained and contains feldspar phenocrysts.

Six zircon were analyzed from sample 08JW131 (Figure 30) from which three grains yielded ages in the Ordovician (z1, z2, z4), two were in the Cretaceous (z3, z6),

and one in the Oligocene (z5). None of the zircon dates overlapped within error and they are interpreted to be detrital zircon in the case of the Ordovician grains or metamorphic/ hydrothermal in the case of the anomalously younger Cretaceous/Tertiary grains. No geologically meaningful age can be interpreted with confidence for this sample. There have been detrital zircon grains for this age reported in the Vinini Formation and this may be the source of the detrital zircon in this sample (Gehrels et al., 2000).

Table 1. Isotopic Data and Ages for Eight Volcanic or Intrusive Igneous Rock Samples.

U-Th-Pb isotopic data

	Compositional Parameters						Radiogenic Isotope Ratios								Isotopic Ages					
Sample	Th/U	^{206}Pb* x10^{-13} mol	mol % ^{206}Pb*	Pb*/Pb$_c$	Pb$_c$ (pg)	^{206}Pb/^{204}Pb	^{208}Pb/^{206}Pb	^{207}Pb/^{206}Pb	% err	^{207}Pb/^{235}U	% err	^{206}Pb/^{238}U	% err	corr. coef.	^{207}Pb/^{206}Pb	±	^{207}Pb/^{235}U	±	^{206}Pb/^{238}U	±
(a)	(b)	(c)	(c)	(c)	(c)	(d)	(e)	(e)	(f)	(e)	(f)	(e)	(f)		(g)	(f)	(g)	(f)	(g)	(f)
08JW131																				
z1	0.420	1.7160	99.48%	57.2	0.74	3589	0.132	0.056527	0.14	0.594061	0.17	0.076220	0.06	0.683	473.1	3.1	473.46	0.64	473.52	0.26
z2	0.525	0.8348	99.15%	35.9	0.59	2197	0.165	0.056513	0.21	0.585714	0.24	0.075169	0.07	0.618	472.6	4.6	468.13	0.91	467.22	0.30
z4	0.161	1.0655	98.69%	20.9	1.16	1418	0.051	0.056368	0.29	0.575190	0.33	0.074007	0.07	0.593	466.9	6.5	461.37	1.22	460.25	0.31
z6	0.463	0.2319	97.73%	12.9	0.44	819	0.146	0.047112	0.95	0.087618	1.02	0.013488	0.11	0.654	54.9	22.7	85.28	0.83	86.37	0.09
z3	0.221	0.2079	97.12%	9.5	0.51	646	0.070	0.047156	1.03	0.073898	1.10	0.011366	0.10	0.723	57.1	24.7	72.39	0.77	72.85	0.07
z5	0.557	0.1003	95.09%	6.0	0.43	379	0.178	0.046132	2.18	0.026313	2.29	0.004137	0.20	0.568	4.5	52.5	26.37	0.60	26.61	0.05
08JW691																				
z1	0.421	11.0614	99.85%	204.0	1.32	12788	0.133	0.051163	0.07	0.278094	0.11	0.039421	0.06	0.807	248.2	1.7	249.14	0.24	249.25	0.14
z5	0.411	6.9563	99.86%	205.4	0.83	12909	0.130	0.051132	0.08	0.277915	0.12	0.039420	0.06	0.767	246.8	1.8	249.00	0.26	249.24	0.14
z4	0.395	7.7025	99.85%	200.2	0.93	12637	0.125	0.051170	0.06	0.277918	0.10	0.039391	0.05	0.856	248.5	1.5	249.00	0.23	249.06	0.13
z2	0.420	8.0267	99.87%	227.9	0.86	14283	0.133	0.051195	0.05	0.277126	0.10	0.039260	0.05	0.913	249.6	1.2	248.38	0.21	248.24	0.13
z3	0.394	10.9567	99.87%	233.8	1.14	14757	0.125	0.051168	0.06	0.276676	0.10	0.039217	0.05	0.871	248.4	1.4	248.02	0.22	247.98	0.13
08JW534																				
z6	0.449	1.6603	99.22%	38.0	1.08	2377	0.142	0.051091	0.22	0.277746	0.26	0.039428	0.06	0.618	244.9	5.1	248.87	0.56	249.28	0.15
z7	0.388	1.7363	99.56%	66.2	0.63	4201	0.123	0.051145	0.13	0.277904	0.17	0.039409	0.06	0.695	247.4	3.1	248.99	0.37	249.17	0.14
z1	0.417	2.3956	99.63%	79.8	0.73	5018	0.132	0.051102	0.16	0.277616	0.19	0.039401	0.06	0.545	245.4	3.7	248.76	0.41	249.12	0.16
z9	0.614	0.7744	98.43%	19.7	1.01	1188	0.195	0.051154	0.42	0.277774	0.46	0.039383	0.07	0.623	247.8	9.8	248.89	1.02	249.01	0.17
z4	0.376	1.5104	99.59%	70.9	0.51	4508	0.119	0.051189	0.13	0.277906	0.16	0.039375	0.05	0.698	249.3	3.0	249.00	0.36	248.96	0.13
z8	0.458	0.9515	98.65%	21.9	1.07	1374	0.145	0.051086	0.37	0.277314	0.41	0.039371	0.06	0.616	244.7	8.6	248.52	0.90	248.93	0.16
z3	0.414	1.3329	99.34%	44.7	0.73	2818	0.131	0.051182	0.33	0.277032	0.36	0.039256	0.10	0.489	249.1	7.5	248.30	0.80	248.22	0.23
z2	0.378	2.0505	99.59%	72.2	0.69	4589	0.120	0.051229	0.39	0.277083	0.41	0.039227	0.14	0.277	251.2	9.1	248.34	0.90	248.04	0.33
z10	0.397	0.9717	99.02%	29.8	0.79	1896	0.126	0.051116	0.29	0.272660	0.32	0.038687	0.06	0.591	246.1	6.6	244.82	0.70	244.69	0.15
08JW71																				
z2	0.705	0.7098	98.78%	26.0	0.72	1530	0.223	0.051111	0.47	0.277186	0.51	0.039333	0.09	0.446	245.8	10.9	248.42	1.11	248.70	0.22
z1	0.502	0.4325	98.64%	22.0	0.49	1365	0.162	0.048865	0.59	0.120232	0.64	0.017845	0.07	0.739	141.3	13.8	115.28	0.69	114.02	0.08
z8	0.556	0.2047	97.88%	14.2	0.36	877	0.178	0.048239	0.94	0.107096	1.00	0.016102	0.10	0.684	111.0	22.1	103.31	0.98	102.97	0.10
z9	0.435	0.1940	97.26%	10.6	0.45	680	0.139	0.048014	1.09	0.099831	1.17	0.015080	0.10	0.706	100.0	25.9	96.62	1.07	96.49	0.10
z7	0.481	0.1094	91.43%	3.2	0.84	217	0.154	0.047819	3.27	0.095478	3.43	0.014481	0.21	0.761	90.3	77.6	92.59	3.04	92.68	0.20
z10	0.354	0.0970	96.10%	7.2	0.32	477	0.112	0.047199	2.42	0.093219	2.53	0.014324	0.14	0.815	59.3	57.7	90.50	2.19	91.68	0.12
z6	0.420	0.2482	98.48%	19.3	0.31	1226	0.135	0.047998	0.56	0.093274	0.61	0.014094	0.08	0.610	99.2	13.2	90.55	0.52	90.22	0.07

Table 1. Isotopic Data and Ages for Eight Volcanic or Intrusive Igneous Rock Samples. (Continued)

	Compositional Parameters						Radiogenic Isotope Ratios								Isotopic Ages					
Sample	Th/U	$^{206}Pb^*$ x10^{-13} mol	mol % $^{206}Pb^*$	Pb^*/Pb_c	Pb_c (pg)	$^{206}Pb/^{204}Pb$	$^{208}Pb/^{206}Pb$	$^{207}Pb/^{206}Pb$	% err	$^{207}Pb/^{235}U$	% err	$^{206}Pb/^{238}U$	% err	corr. coef.	$^{207}Pb/^{206}Pb$	±	$^{207}Pb/^{235}U$	±	$^{206}Pb/^{238}U$	±
(a)	(b)	(c)	(c)	(c)	(c)	(d)	(e)	(e)	(f)	(e)	(f)	(e)	(f)		(g)	(f)	(g)	(f)	(g)	(f)
08JW462																				
z5	0.188	3.2877	99.74%	104.9	0.72	7031	0.060	0.049799	0.10	0.183857	0.13	0.026777	0.05	0.735	185.6	2.3	171.37	0.20	170.34	0.09
z3	0.184	3.0371	99.75%	111.1	0.62	7459	0.059	0.049437	0.10	0.175047	0.13	0.025680	0.06	0.739	168.6	2.3	163.79	0.20	163.46	0.09
z2	0.207	2.9700	99.71%	96.7	0.71	6442	0.067	0.049954	0.20	0.175670	0.22	0.025505	0.07	0.436	192.9	4.6	164.33	0.33	162.35	0.11
z4	0.152	2.9431	99.67%	83.0	0.80	5623	0.049	0.049458	0.11	0.173412	0.14	0.025430	0.06	0.729	169.6	2.5	162.38	0.21	161.88	0.09
z1	0.211	2.4592	99.64%	76.9	0.74	5131	0.067	0.049134	0.35	0.170083	0.36	0.025106	0.10	0.214	154.2	8.2	159.49	0.53	159.85	0.15
08JW661																				
z2	0.233	3.6491	99.82%	159.0	0.53	10509	0.074	0.049862	0.07	0.195102	0.11	0.028379	0.06	0.843	188.6	1.6	180.97	0.18	180.39	0.10
z4	0.224	2.6032	99.87%	223.4	0.27	14791	0.072	0.049620	0.06	0.174860	0.11	0.025558	0.06	0.879	177.2	1.4	163.63	0.16	162.69	0.09
z7	0.171	2.3536	98.66%	20.4	2.63	1389	0.054	0.049345	0.38	0.173245	0.42	0.025463	0.09	0.510	164.3	8.9	162.23	0.62	162.09	0.14
z1	0.263	1.9498	99.80%	140.9	0.32	9243	0.084	0.049248	0.08	0.172638	0.12	0.025424	0.06	0.830	159.7	1.8	161.71	0.18	161.85	0.09
z6	0.196	2.2563	99.83%	162.2	0.32	10840	0.063	0.049366	0.06	0.173007	0.11	0.025418	0.05	0.899	165.2	1.5	162.03	0.16	161.81	0.09
z5	0.170	2.0060	99.82%	150.5	0.30	10136	0.054	0.049231	0.07	0.172523	0.11	0.025416	0.06	0.844	158.9	1.7	161.61	0.17	161.79	0.09
z3	0.182	2.5711	99.87%	208.2	0.28	13972	0.058	0.049257	0.06	0.172549	0.11	0.025406	0.06	0.870	160.1	1.5	161.63	0.16	161.73	0.09
09JW891																				
z2	0.549	1.3077	99.71%	104.7	0.32	6357	0.175	0.049216	0.12	0.172737	0.15	0.025455	0.06	0.708	158.2	2.7	161.79	0.22	162.04	0.09
z4	0.600	0.5677	99.16%	36.9	0.39	2225	0.191	0.049296	0.26	0.172867	0.29	0.025433	0.06	0.607	161.9	6.0	161.90	0.44	161.90	0.10
z3	0.639	0.7841	99.42%	53.9	0.38	3209	0.203	0.049262	0.20	0.172743	0.23	0.025433	0.06	0.586	160.3	4.6	161.80	0.34	161.90	0.09
z6	0.629	0.6640	99.41%	52.5	0.33	3130	0.201	0.049329	0.16	0.172977	0.20	0.025432	0.06	0.731	163.5	3.8	162.00	0.30	161.90	0.10
z7	0.664	0.6246	99.03%	32.4	0.50	1921	0.212	0.049303	0.29	0.172841	0.33	0.025426	0.05	0.757	162.3	6.9	161.88	0.49	161.86	0.08
z5	0.553	0.5481	99.02%	31.0	0.45	1897	0.176	0.049179	0.43	0.172363	0.47	0.025419	0.06	0.701	156.4	10.1	161.47	0.71	161.81	0.10
z1	0.569	1.4559	99.68%	95.9	0.39	5797	0.181	0.049279	0.11	0.172699	0.15	0.025417	0.06	0.727	161.1	2.6	161.76	0.22	161.80	0.09
08JW391																				
z1	1.199	0.8226	98.83%	30.3	0.80	1589	0.381	0.049187	0.35	0.172373	0.38	0.025417	0.06	0.592	156.8	8.1	161.48	0.57	161.80	0.10
z2	0.630	1.2092	99.12%	35.5	0.88	2125	0.201	0.049282	0.31	0.172631	0.34	0.025405	0.07	0.491	161.3	7.4	161.70	0.51	161.73	0.11
z3	1.145	0.5792	98.22%	19.6	0.86	1043	0.364	0.049131	0.87	0.172077	0.93	0.025402	0.10	0.597	154.1	20.4	161.22	1.38	161.71	0.16
z5	0.516	0.1954	95.81%	7.0	0.70	444	0.166	0.049784	1.36	0.174267	1.45	0.025388	0.12	0.805	184.9	31.6	163.11	2.19	161.62	0.19
z4	1.136	1.2406	98.33%	20.9	1.73	1115	0.361	0.049064	0.45	0.171726	0.49	0.025385	0.06	0.711	150.9	10.6	160.92	0.73	161.60	0.10

(a) z1, z2 etc. are labels for fractions composed of single zircon grains or fragments; all fractions annealed and chemically abraded after Mattinson (2005).

(b) Model Th/U ratio calculated from radiogenic 208Pb/206Pb ratio and 207Pb/235U age.

(c) Pb* and Pbc represent radiogenic and common Pb, respectively; mol % $^{206}Pb^*$ with respect to radiogenic, blank and initial common Pb.

(d) Measured ratio corrected for spike and fractionation only. Mass fractionation correction of 0.18 ± 0.02 (1-sigma) %/amu (atomic mass unit) was applied to all single-collector Daly analyses, based on analysis of NBS-981 and NBS-982.

(e) Corrected for fractionation, spike, and common Pb; all common Pb was assumed to be procedural blank: 206Pb/204Pb = 18.60 ± 0.80%; 207Pb/204Pb = 15.69 ± 0.32%; 208Pb/204Pb = 38.51 ± 0.74% (all uncertainties 1-sigma). 206Pb/238U and 207Pb/206Pb ratios corrected for initial disequilibrium in 230Th/238U using Th/U [magma] = 4.

(f) Errors are 2-sigma, propagated using the algorithms of Schmitz and Schoene (2007) and Crowley et al. (2007).

(g) Calculations are based on the decay constants of Jaffey et al. (1971). 206Pb/238U and 207Pb/206Pb ages corrected for initial disequilibrium in 230Th/238U using Th/U [magma] = 4.

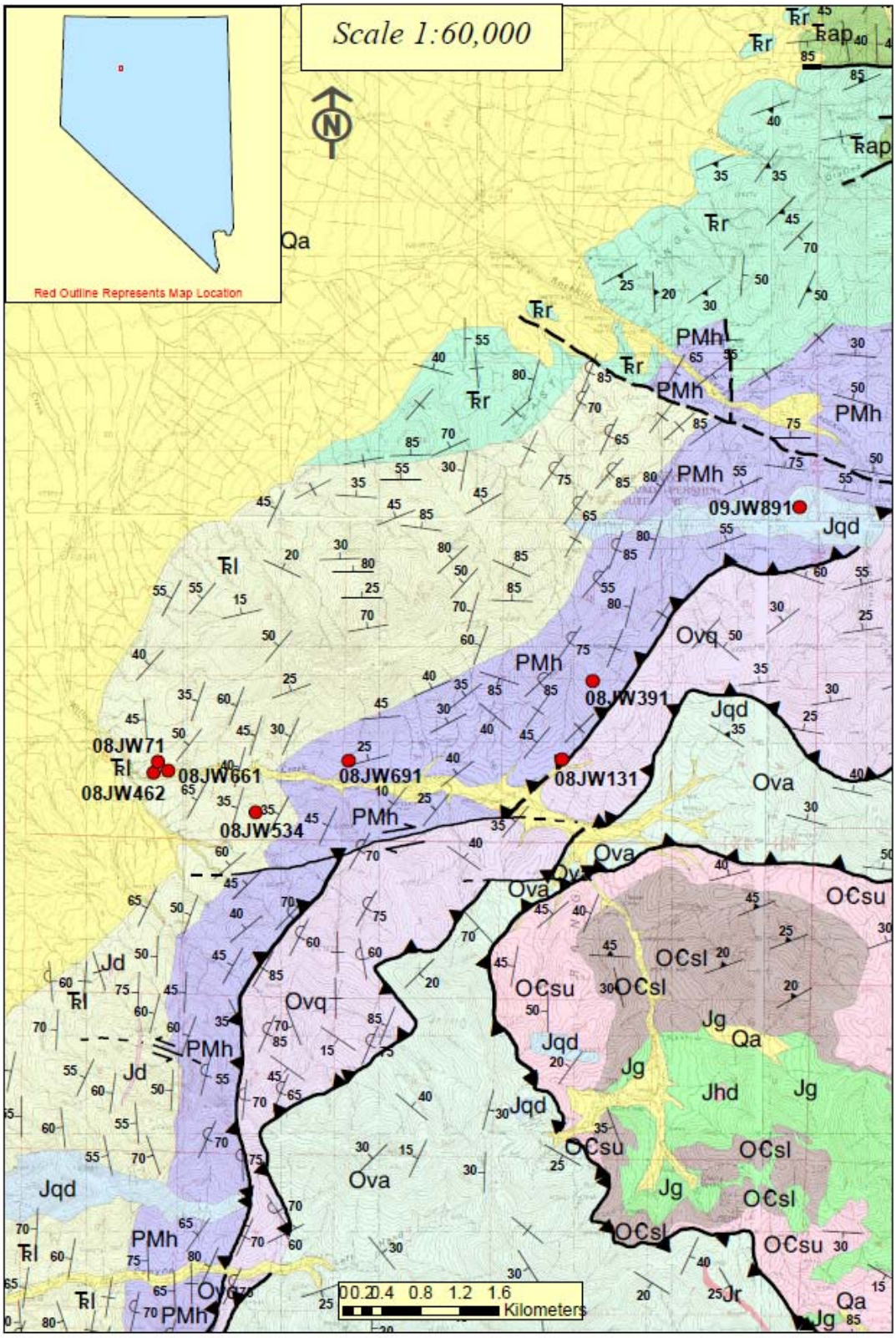

Figure 25. Geologic Map Showing Location of All Geochronology Samples. View Legend on Plate 1 for Unit Names Descriptions and Map Symbols.

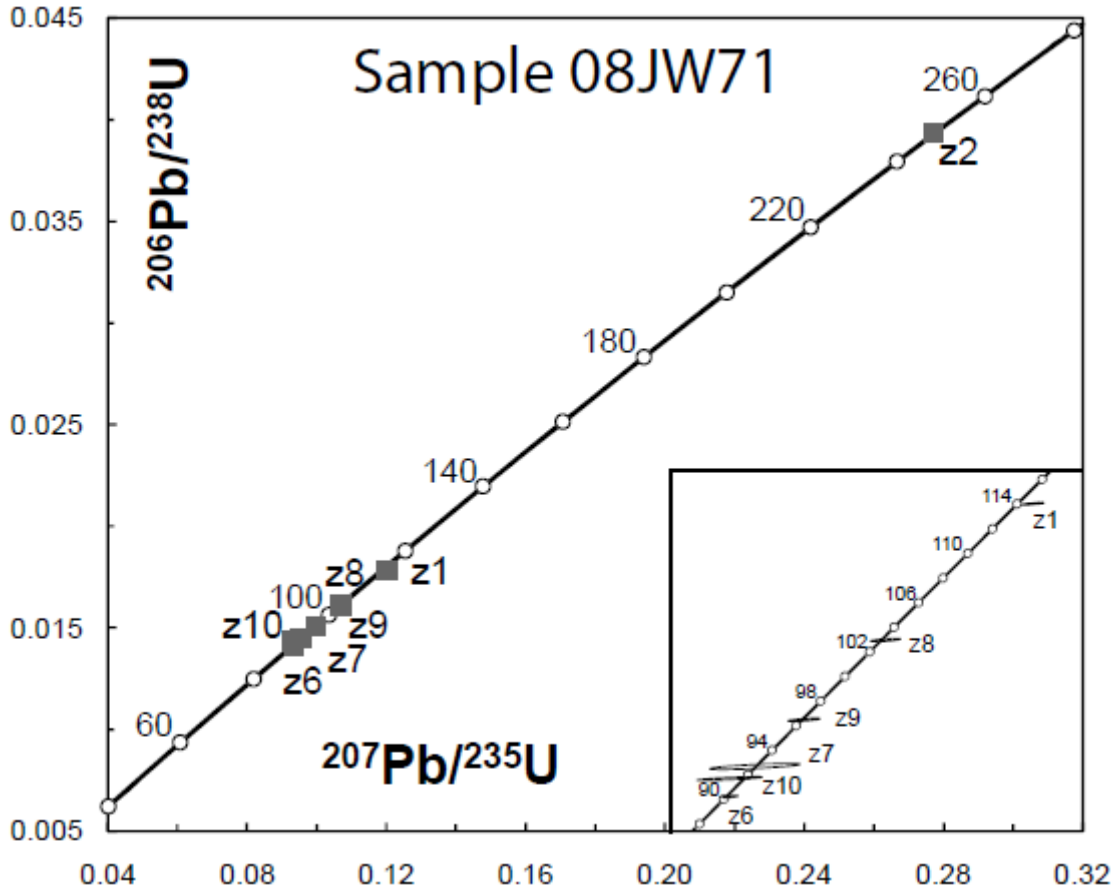

Figure 26. Sample 08JW71. Concordia Diagram with Individual Zircon Analyses Plotted as Grey Squares. Inset Shows Details of Cretaceous Metamorphic or Hydrothermal Zircon.

Figure 27. Field Photograph of Sample 08JW534, a White Tuff Interbedded with Grey Phyllite in the Upper Inskip Formation.

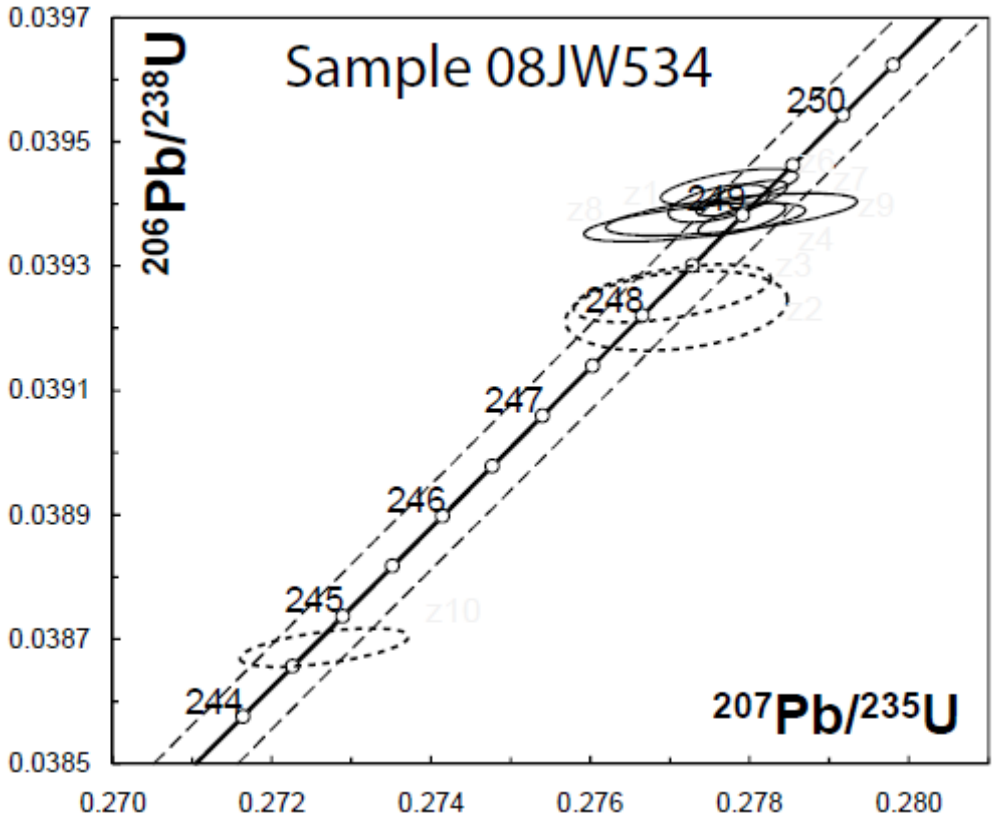

Figure 28a. Sample 08JW534. Concordia Diagram with Error Ellipses for Individual Zircon Analyses. Solid Ellipses Are Zircon Used in the Weighted Mean Age Calculation for the Sample. Dashed Ellipses Are Zircon Not Used in the Age Calculation. Dashed Lines Define the Error Associated within the Concordia Calculation.

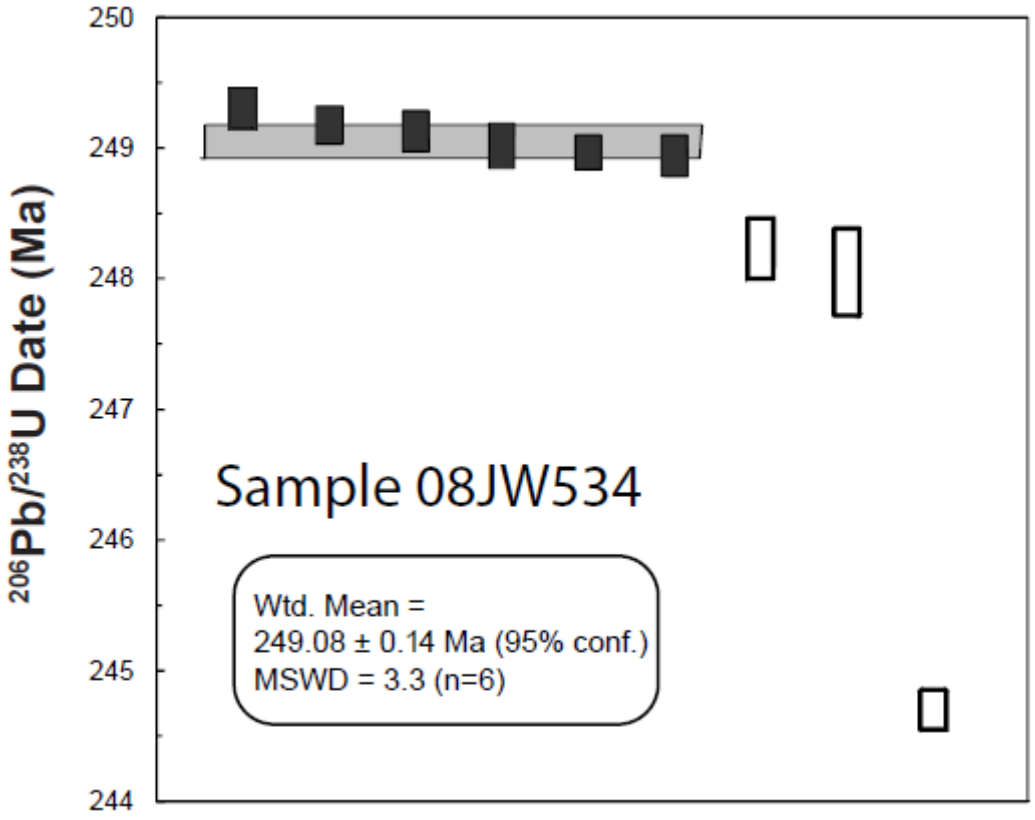

Figure 28b. Ranked 206 Pb/238 U Age Plot of Analysis from Sample 08JW534. Black Boxes Are Zircon Used in the Age Calculation for the Sample. White Boxes Are Zircon Not Used in the Age Calculation. Grey Box Illustrates the Weighted Mean Age of the Sample and Its Associated Error.

Figure 29. Field Photo of Location for Sample 08JW131, Interpreted to be a Tuff. View to the West, Compass for Scale.

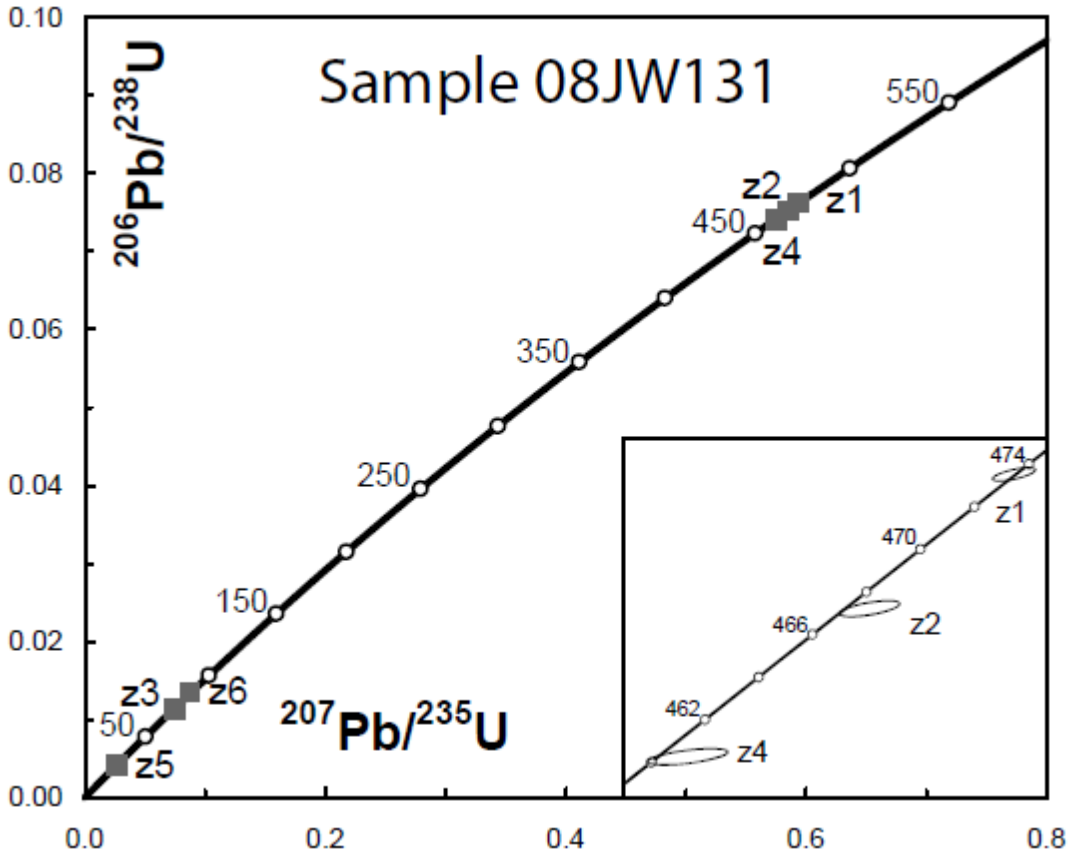

Figure 30. Sample 08JW131. Concordia Diagram with Individual Zircon Analyses Plotted as Grey Squares. Inset Shows Details of the Ordovician Detrital Zircon.

Age of Deformation

Due to the fact that the Triassic rocks of the Upper Inskip Formation and the Rochester Member of the Koipato Group are deformed to the same degree as the Upper Paleozoic rocks of the Lower Inskip Formation, deformation occurred after the deposition of the Early Triassic rocks. The presence of intrusions ranging from strongly deformed to non-deformed offers the opportunity to generate additional timing constraints on deformation.

Samples from four sills (two strongly deformed, two weakly to non-deformed) and one small stock were collected for geochronology. Results of the U-Pb zircon analyses are reported in Table 1 and locations are shown in Figure 25. All ages are reported at the 95% confidence interval. Location for each of the samples is reported in the WGS 1984 datum, and the UTM zone 11 N projection.

Sample 08JW391- slightly deformed sill from Lower Inskip Formation – UTM 0424111E, 4495830N

Sample 08JW391 was collected from the lower half of the Lower Inskip Formation and is a felsic sill that has only a very slight mineral alignment. The sample was collected to constrain the minimum age of the deformation.

Five single zircon grains were analyzed from sample 08JW391 (Figure 31a-b). These five zircon yielded 206Pb/238U dates with a weighted mean date of 161. 76 +/-

0.11 Ma (MSWD = 2.3). The age places the intrusion of the felsic sill in the late Middle Jurassic.

Sample 08JW691- deformed sill from Lower Inskip Formation

– UTM 0421609E, 4495016N

Another sample collected in the Lower Inskip Formation but near the top of the section is sample 08JW691, which is a highly deformed quartz diorite sill with the distinctive large feldspar megacrysts. The sample has been exposed to all of the deformation and was collected to generate a maximum age for the deformation.

Five single zircon crystals were analyzed from sample 08JW691 (Figure 32a-b). These crystals yielded 206Pb/238U dates ranging from 249.34 +/- 0.14 Ma to 248.07 +/- 0.13 Ma. The weighted mean date was calculated using the oldest three zircon grains, which yielded an age of 249.27 +/- 0.27 Ma (MSWD = 2.5). The two zircon grains not used in the calculation were interpreted to have had slight Pb loss or reflect the presence of thin metamorphic rims.

Sample 08JW462- deformed sill from Upper Inskip Formation

– UTM 0419932E, 4494990N

Sample 08JW462 is strongly deformed with well-developed mineral alignment and penetrative foliation. This sample was collected near the top of the exposed Upper

Inskip Formation and is a felsic sill/dike that cuts across bedding obliquely in places. The purpose of this sample is to give a maximum age for the penetrative deformation.

Five single zircon grains were analyzed from sample 08JW462 (Figure 33). 206Pb/238U dates ranged from 170.41 +/- 0.09 Ma to 159.91 +/- 0.15 Ma. None of the dates obtained overlapped within error. Zircon systematics may have been affected by a combination of inheritance and/or the growth of metamorphic/hydrothermal zircon.

Sample 08JW661- slightly deformed sill from Upper Inskip Formation – UTM 0419764E, 4494913N

Sample 08JW661 was also collected near the top of the Upper Inskip Formation and is a relatively undeformed felsic sill, with the only evidence of deformation being undulose extinction of quartz observed petrographically (Figure 24). The sample was collected to give a minimum age of the deformation.

Seven zircon grains were analyzed from sample 08JW661 (Figure 34 a-b). Four grains yielded 206Pb/238U dates with a weighted mean date of 161.86 +/- 0.04 Ma (MSWD = 1.0). This is the interpreted age of the sample. Two grains were slightly older (162.69 Ma and 162.09 Ma) than the four grains used for the age of the sample and are interpreted to represent antecrysts. One zircon was significantly older and is interpreted to reflect xenocrystic inheritance.

Sample 09JW891- nondeformed small stock

– UTM 0426178E, 4497435N

Sample 09JW891 was collected from an undeformed quartz diorite pluton that cross cuts the contact between the Upper Inskip Formation and the Lower Inskip Formation, and the contact between the Lower Inskip Formation and the Valmy Formation. The pluton is located just south of Rockhill Canyon. This sample was collected to provide a minimum age on the penetrative deformation as well as a minimum age for the juxtaposition of the Inskip Formation with the Valmy Formation.

Seven zircon grains were analyzed from sample 09JW891 (Figure 35a-b). Six grains yielded 206Pb/238U dates with a weighted mean date 161.86 +/- 0.04 Ma (MSWD = 0.9), which is interpreted as the age of the sample. The one zircon was not used for the age calculation is interpreted as an older (162.04 Ma) antecryst.

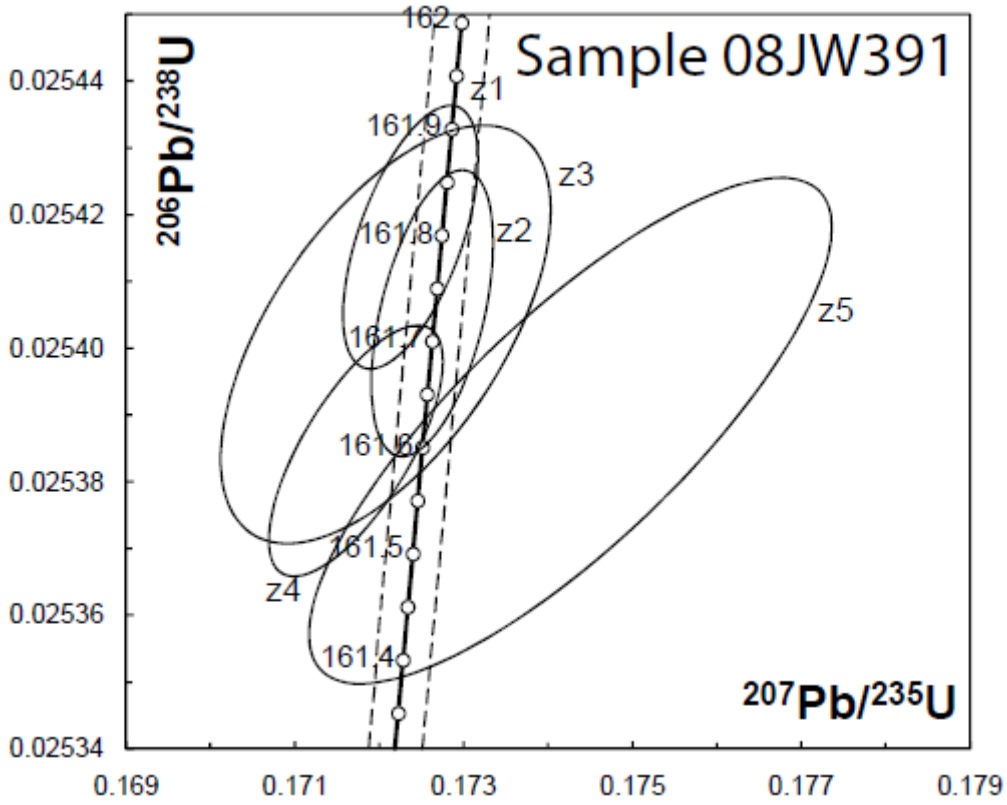

Figure 31a. Concordia Diagram Showing Results from Sample 08JW391 Zircon Analyses. Solid Ellipses Are Zircon Used in the Weighted Mean Age Calculation for the Sample. Dashed Lines Define the Error Associated Within the Concordia Calculation.

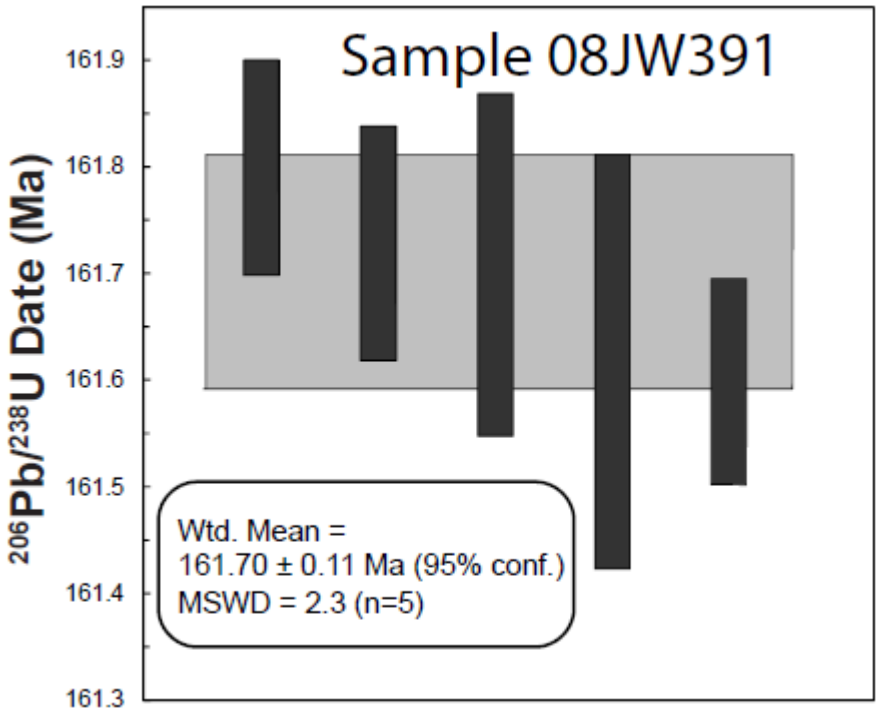

Figure 31b. Ranked 206Pb/238U Age Plot for Sample 08JW391. Black Boxes Are Zircon Used in the Weighted Mean Age Calculation for the Sample. Grey Box Shows the Calculated Age of the Sample and Its Associated Error.

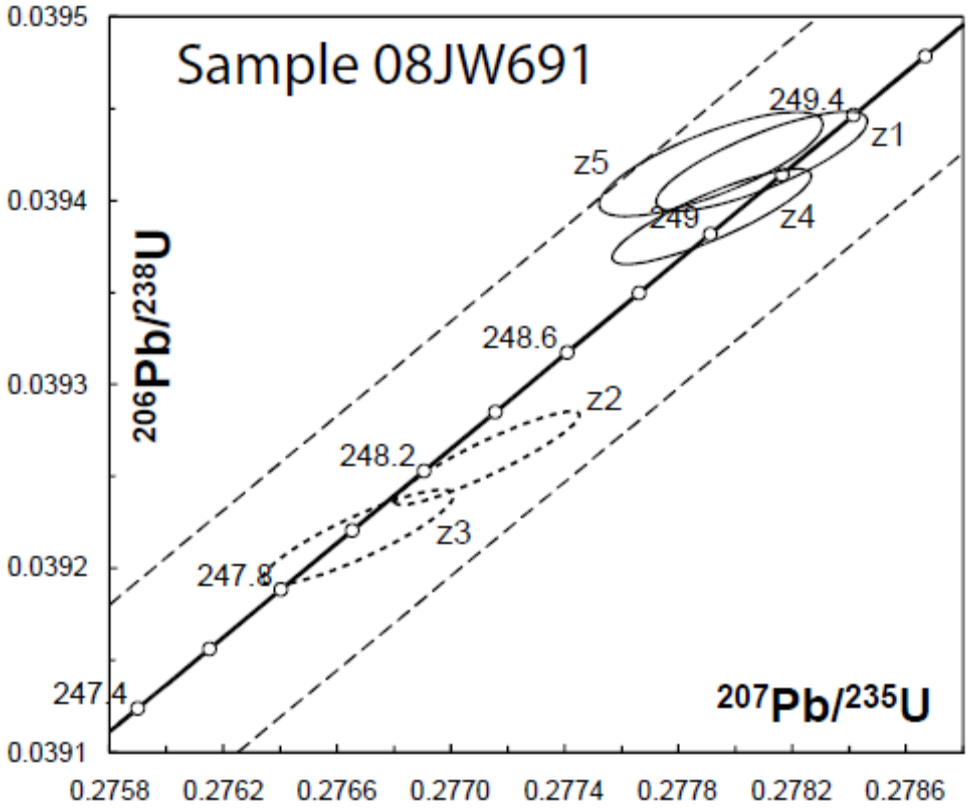

Figure 32a. Concordia Diagram Showing Results from Sample 08JW691 Zircon Analyses. Solid Ellipses Are Zircon Used in the Weighted Mean Age Calculation for the Sample. Dashed Ellipses Are Zircon Not Used in the Age Calculation. Dashed Lines Define the Error Associated Within the Concordia Calculation.

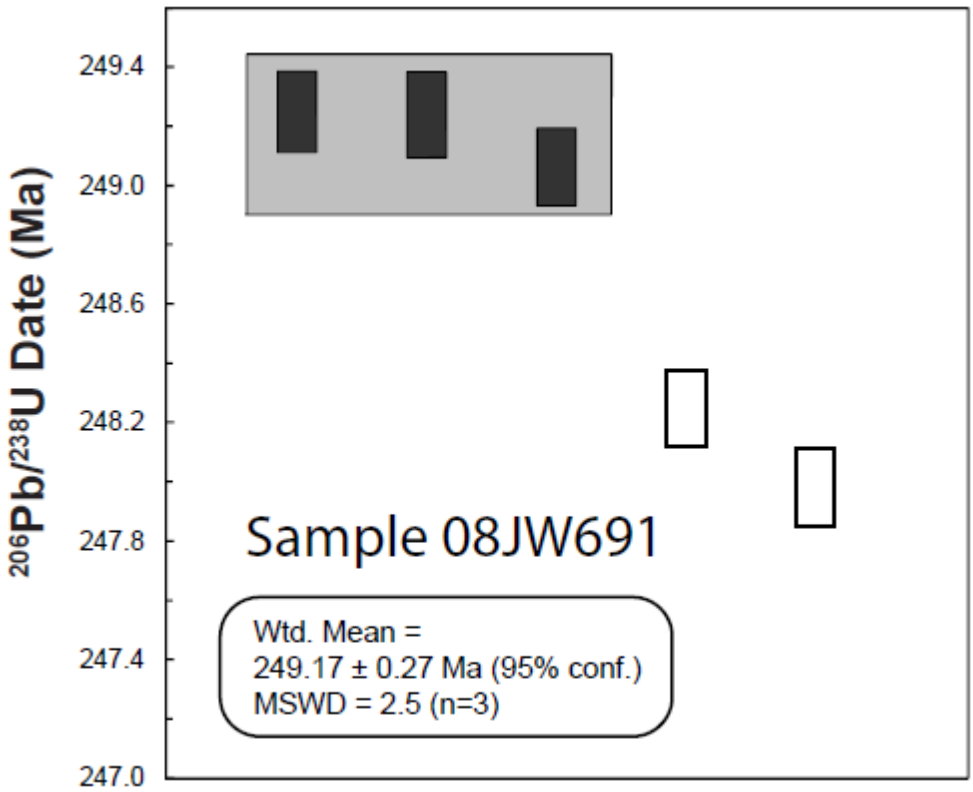

Figure 32b. Ranked 206Pb/238U Age Plot for Sample 08JW691. Black Boxes Are Zircon Used in the Weighted Mean Age Calculation for the Sample; White Boxes Are Zircon Not Used in the Age Calculation. Grey Box Shows the Calculated Age of the Sample and Its Associated Error.

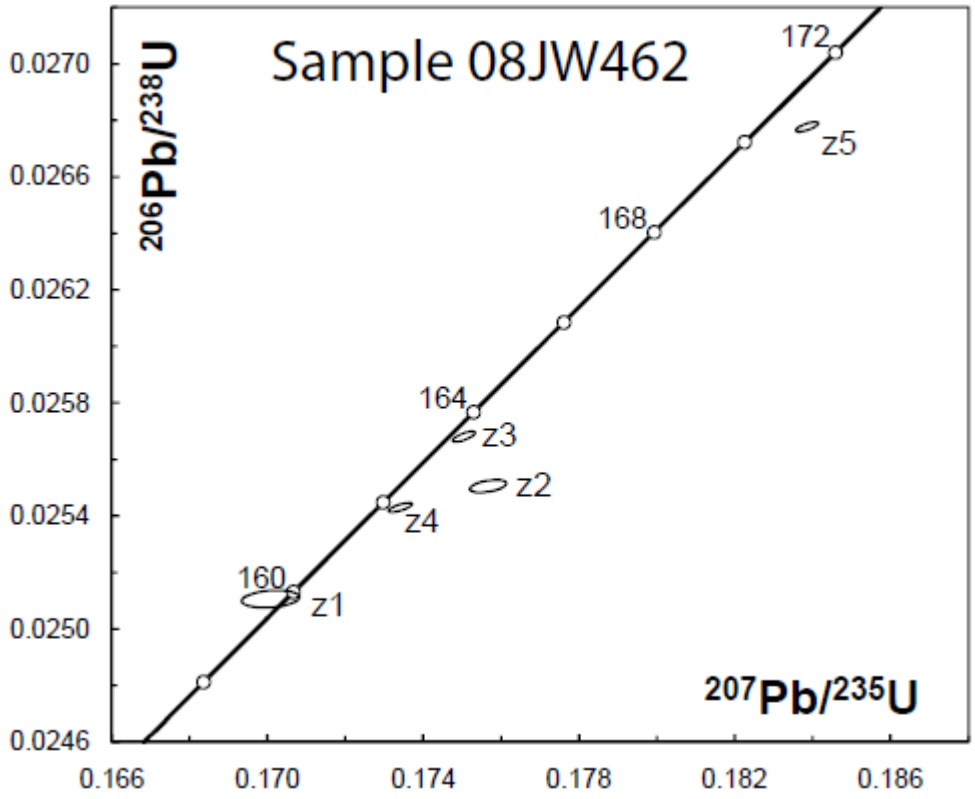

Figure 33. Concordia Diagram Showing Results from Sample 08JW462 Zircon Analyses.

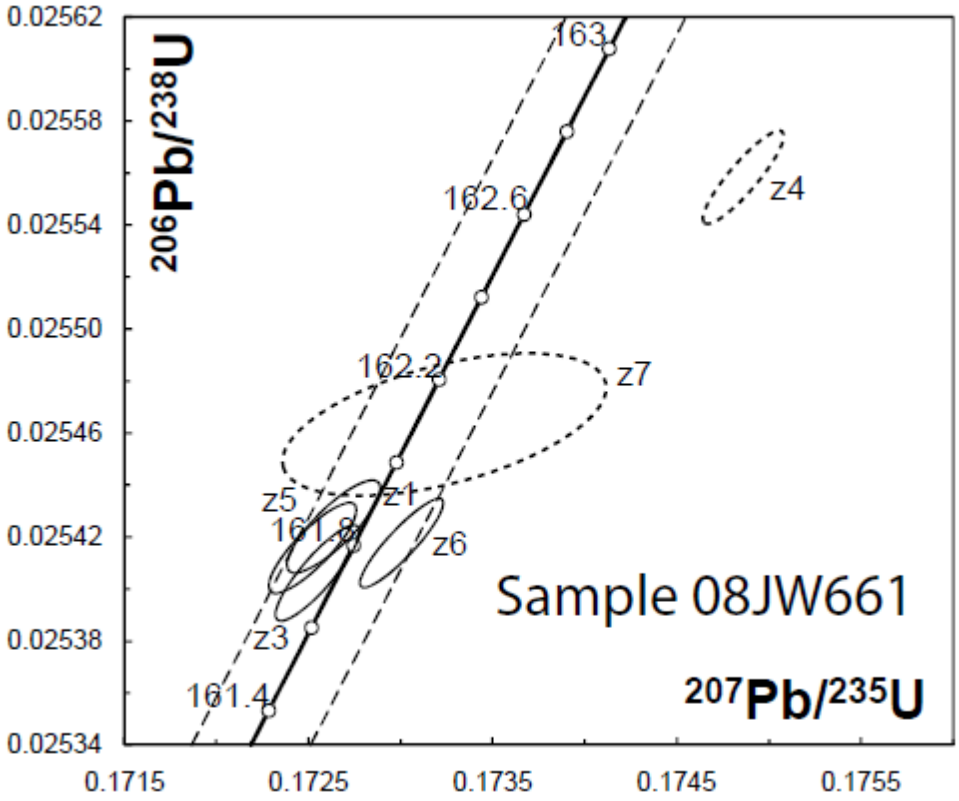

Figure 34a. Concordia Diagram Showing Results from Sample 08JW661 Zircon Analyses. Solid Ellipses Are Zircon Used in the Weighted Mean Age Calculation for the Sample. Dashed Ellipses Are Zircon Not Used in the Age Calculation. Dashed Lines Define the Error Associated Within the Concordia Calculation.

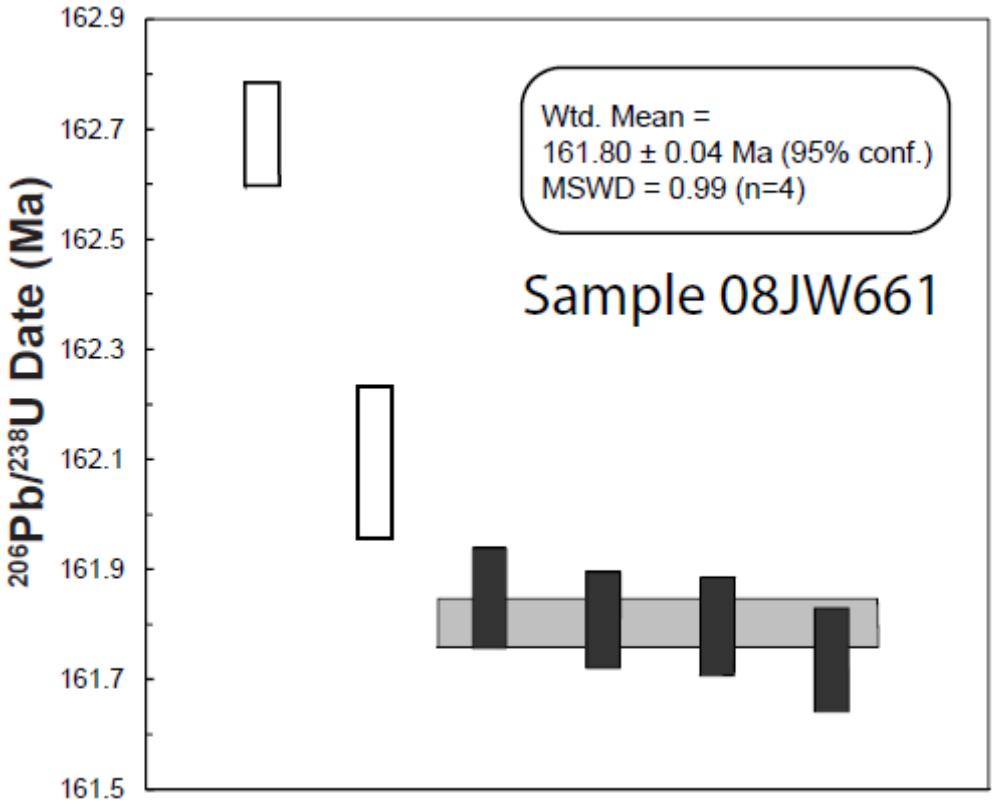

Figure 34b. Ranked 206Pb/238U Age Plot for Sample 08JW661. Black Boxes Are Zircon Used in the Weighted Mean Age Calculation for the Sample. White Boxes Are Zircon Not Used in the Age Calculation. Grey Box Shows the Calculated Age of the Sample and Its Associated Error.

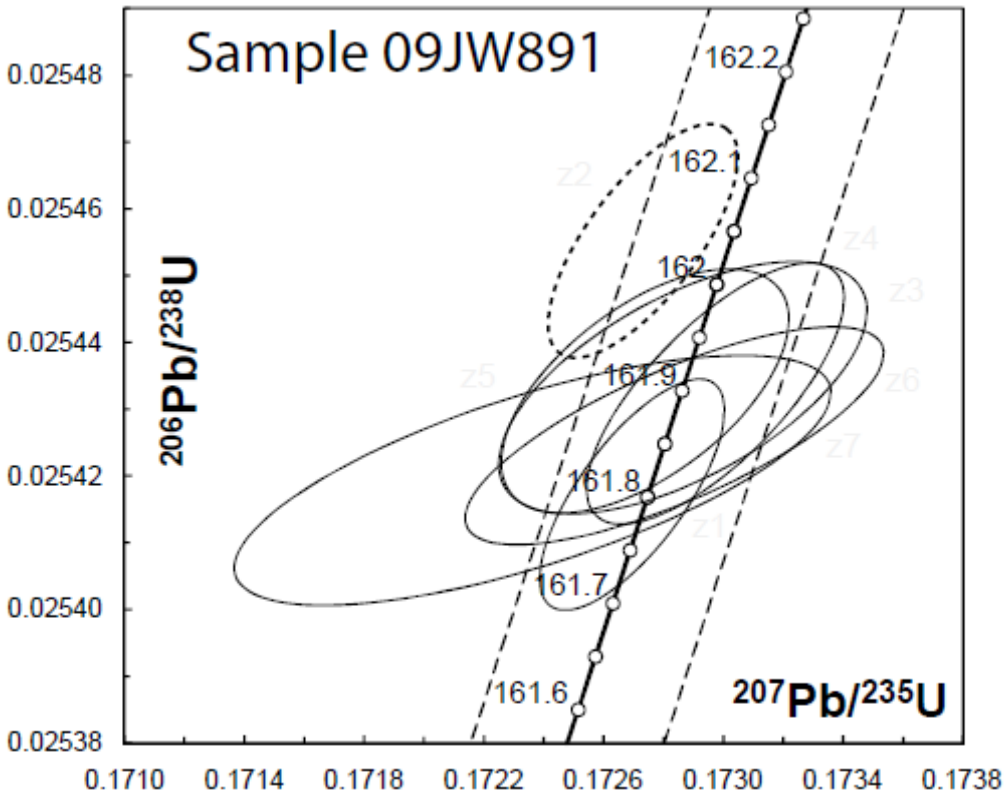

Figure 35a. Concordia Diagram Showing Results from Sample 09JW891 Zircon Analyses. Solid Ellipses Are Zircon Used in the Weighted Mean Age Calculation for the Sample. Dashed Ellipses Are Zircon Not Used in the Age Calculation. Dashed Lines Define the Error Associated Within the Concordia Calculation.

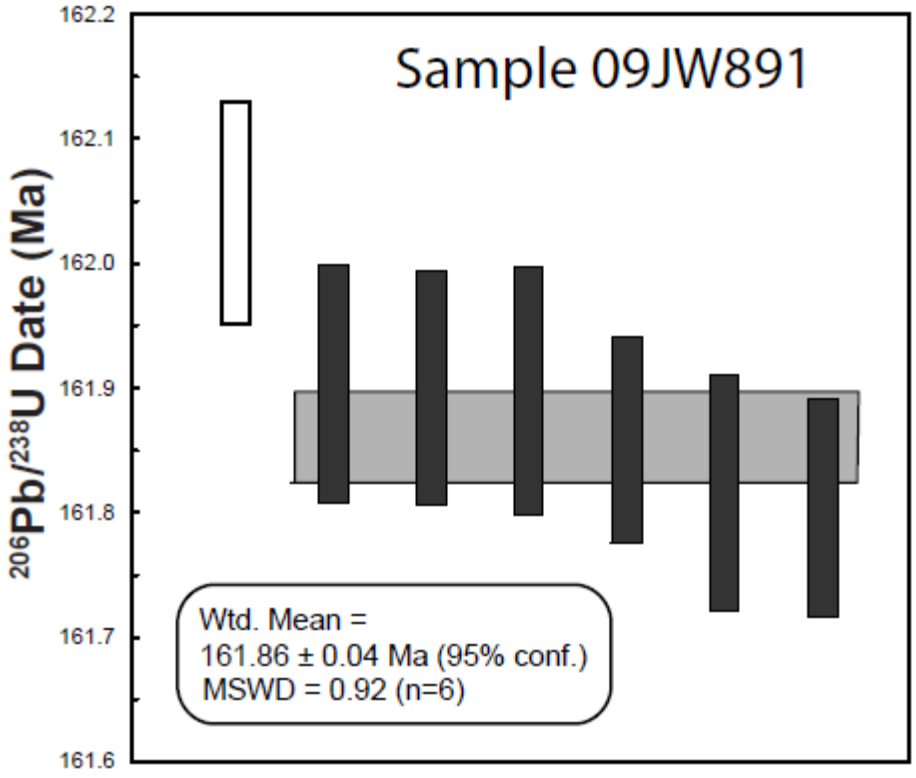

Figure 35b. Ranked 206Pb/238U Age Plot for Sample 09JW891. Black Boxes Are Zircon Used in the Weighted Mean Age Calculation for the Sample. White Boxes Are Zircon Not Used in the Age Calculation. Grey Box Shows the Calculated Age of the Sample and Its Associated Error.

Stratigraphic Age of Inskip Formation

Interpretation of a new age of Early Triassic for the Upper Inskip Formation is based on the geochronology of the two samples (08JW534 and 08JW71). Because the samples are volcanic, the dates are depositional ages for the stratigraphy. The age provided by sample 08JW534 is the more reliable age; however, the single zircon date from sample 08JW71 is younger than the age of 08JW534 and is also in younger strata. Unfortunately, the data obtained from 08JW131 did not provide a depositional age for the Lower Inskip Formation. The detrital zircon grains can be used as a maximum age for the Lower Inskip Formation, which would be younger than Ordovician. However, in this case, the fossils ranging from Devonian to Pennsylvanian offer a better control on the maximum age of the Lower Inskip Formation. Cross-cutting relationships show the Lower Inskip Formation to be no younger than Early Triassic from sample 08JW691. In addition of this sample being the minimum age constraint for the Lower Inskip Formation, it likely is the hypabyssal equivalent to the volcanic in the Upper Inskip Formation.

Stratigraphic Interpretations

New U-Pb geochronologic data places the age of the Upper Inskip Formation in the Early Triassic. Map relationships show an along-strike contrast between the orientation of the Upper Inskip Formation and the Rochester Member Rhyolite at the contact between the units just south of Rockhill Canyon. Because the Rochester Member

is also interpreted to be of Early Triassic age, the Upper Inskip Formation and the Rochester Member are interpreted to be more closely related than has previously been recognized. One possibility is that the Upper Inskip Formation represents a more sediment rich facies of the Rochester Member, with more interstratified sediments. This is plausible given the fact that rhyolite is viscous and typically forms domes rather than flowing laterally for extended distances. However, the lithology of the Upper Inskip Formation resembles that of the Limerick Member, which is described in the Humboldt Range to be andesite overlain by meta sediments. The Upper Inskip Formation has an abundance of greenstone and amphibolites, which before deformation and metamorphism may have been andesite. In the East Range, the greenstone is interbedded with sediments throughout the unit, whereas the andesite is overlain by the sediments in the Humboldt Range. Additionally, the Limerick Member of the Humboldt Range lacks the variety of sediment types that are present in the Upper Inskip Formation. These variations can be attributed to eruption history and the source of the sediments and environment of deposition in the Limerick Member and the Upper Inskip Formation and may just represent a facies change between the two areas. The Upper Inskip Formation and the Limerick Member are similar and are interpreted to be equivalent.

Furthermore, new mapping and interpretation of satellite imagery suggest the Rochester Member to be in an angular unconformable relationship with the Upper Inskip Formation (Figure 36a-b). This angular unconformity extends across what was previously mapped as the Rockhill Canyon strand of the Willow Creek Thrust and places Rochester Member directly over the Havallah sequence in an unconformable relationship in which the Limerick Member was either not deposited or removed by erosion.

In addition to correlating the Upper Inskip Formation to the Limerick Member, the Lower Inskip Formation is here assigned to the Havallah sequence. Ketner et al. (2000) grouped the Inskip Formation, Havallah sequence, and the Harmony Formation into the same tectono-stratigraphic package, and Fergeson et al. (1951) mapped the Inskip Formation in what was later interpreted by Silberling and Roberts. (1962) to be partly Havallah sequence. The major difference between the Lower Inskip Formation and the Havallah sequence recognized north of Rockhill Canyon is that the Havallah sequence appears to be slightly less deformed than the Lower Inskip Formation. Only Ordovician detrital zircons (Sample 08JW131) have been dated from the Lower Inskip Formation. Based on the fossil evidence for the Lower Inskip Formation, the Ordovician age is clearly too old and the zircon may have been reworked from the Valmy Formation during deposition of the Inskip Formation. Absent of new detailed geochronologic data for the Lower Inskip Formation, the constraints of the fossil data are the best evidence for the age of the Lower Inskip Formation. Fossil ages range from Devonian to Pennsylvanian in the Lower Inskip Formation, similar to the range found in Havallah sequence fossils (Devonian to Permian). Summary Figure 37 illustrates the stratigraphic and structural relationships of the area, including approximate locations for selected fossil and geochronologic samples.

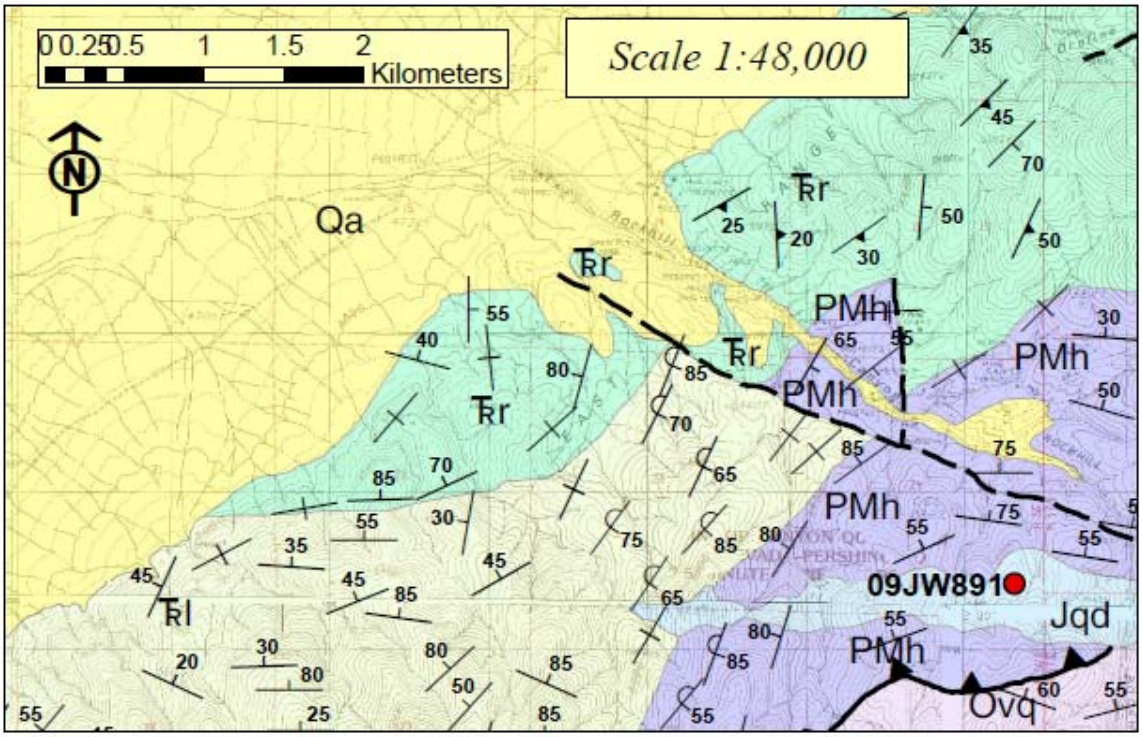

Figure 36a. Geologic Map Showing the Angular Unconformity Between the Rochester Member and the Limerick Member of the Koipato Group. View Legend on Plate 1 for Unit Names Descriptions and Map Symbols.

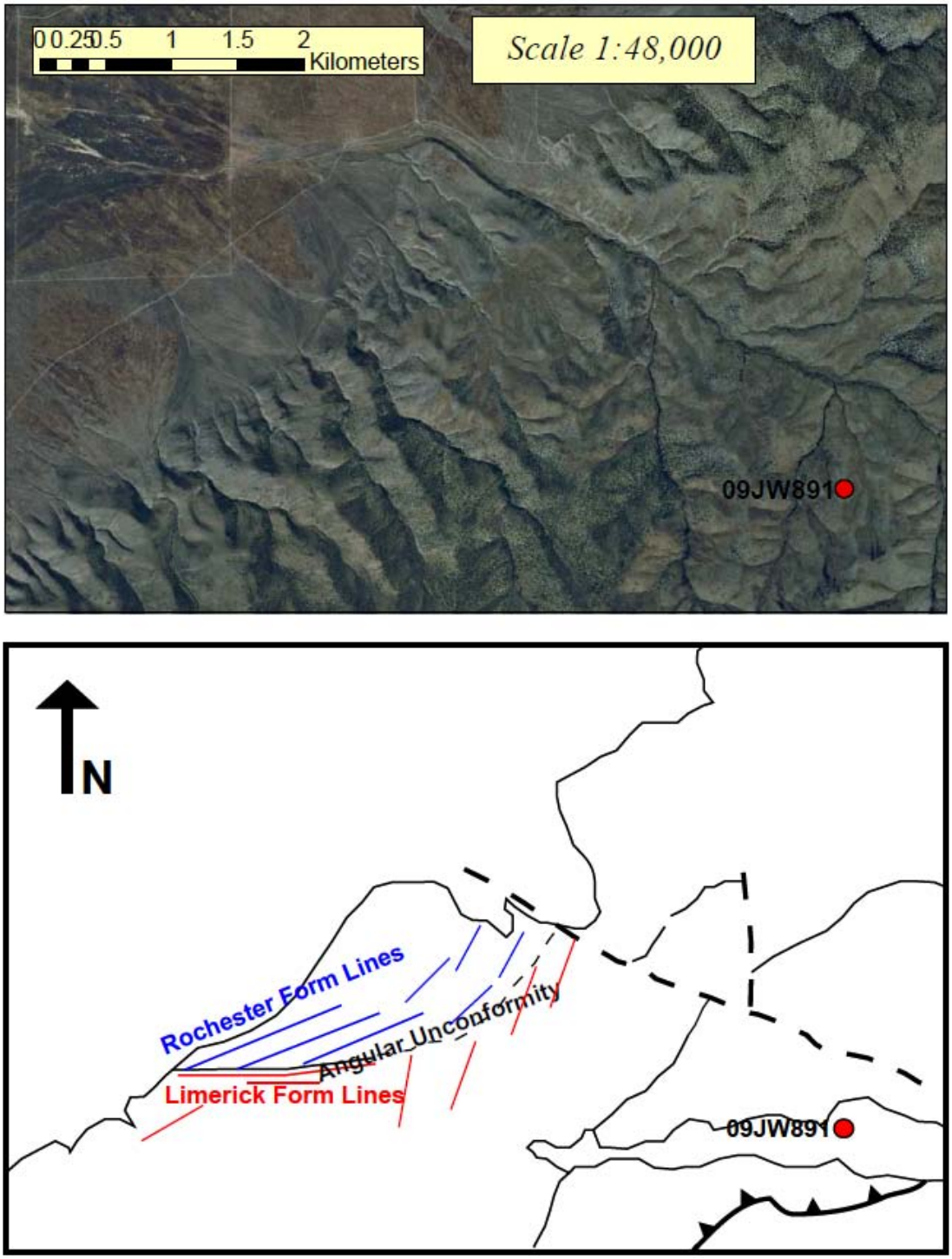

Figure 36b. Arial Photo and Line Drawing of the Same Area as Figure 36a Where the Angular Unconformity Is Visible in the Photo. Blue and Red Form Lines Depict the Orientation of the Beds in the Limerick Member and Rochester Member on Opposite Sides of the Unconformity.

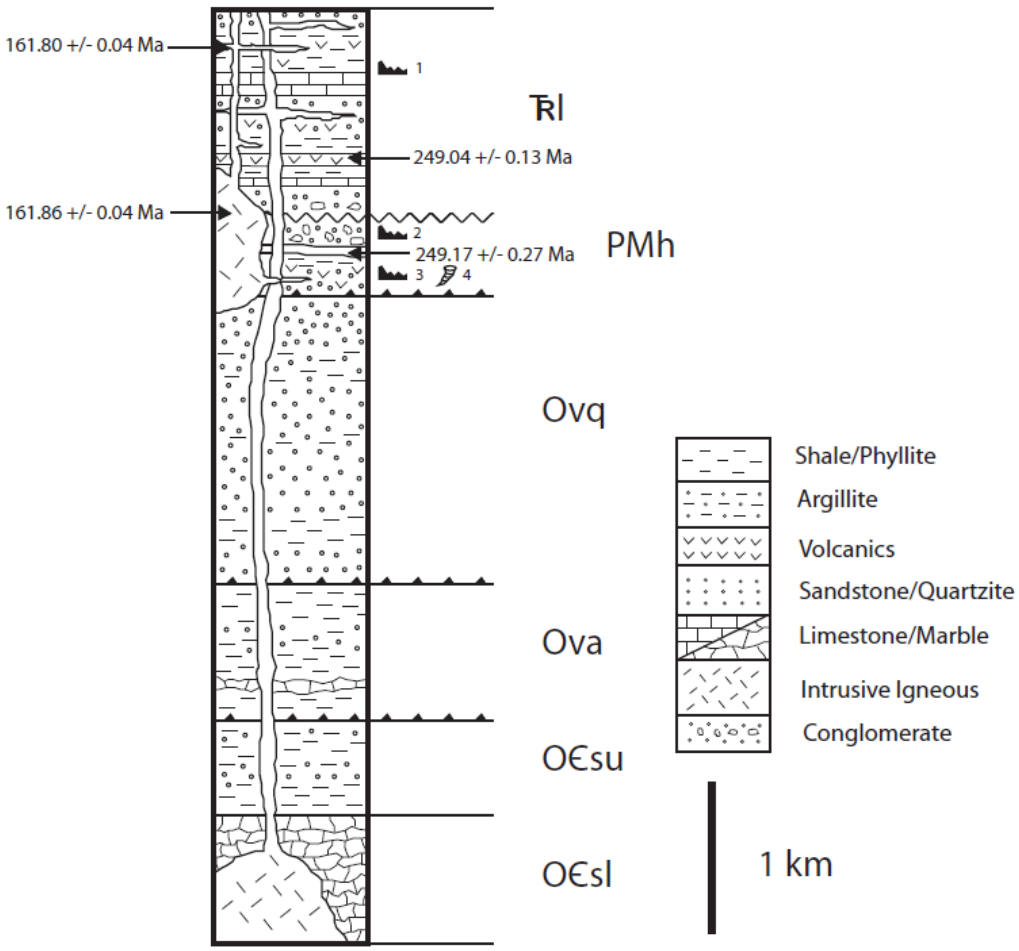

Figure 37. Column Showing the Stratigraphic and Structural Relationships for the Willow Creek Area of the East Range. Ages Displayed at Approximate Stratigraphic Location for Geochronologic Samples. General Fossil Locations Displayed for Conodont and Coral Fossils. Fossils May Be Reworked. (1) Permian Conodont. (2) Pennsylvanian Conodont. (3) Mississippian Conodont. (4) Mississippian Coral.

Timing of Deformation

The purpose of this section is to evaluate and discuss the new age constrains on the deformational history of the Upper and Lower Inskip Formation of the north-central East Range. Five phases of deformation have been recognized (Table 2). Deformation is constrained between the Early Triassic and the Late Middle Jurassic.

Interpretation for the end of the deformation in the area or a minimum age of the deformation is based on the three samples that exhibit very little to no deformation (Samples 08JW391, 08JW661, and 09JW891). Sample 08JW661, which has undulose extinction in the quartz grains, could have undergone the last of the deformation or potentially been exposed to a low grade deformation/metamorphic event not recognized on a broader scale (Figure 24). Sample 08JW391 may have been more susceptible to the deformation because the sill is relatively narrow, approximately 20 cm wide. Whereas the pluton (09JW891) is likely more competent and resistant to deformation because it is a larger more ridged body. Nevertheless, the minimum age for deformation established by the new geochronology is late Middle Jurassic. The maximum age, however, is not as direct. Sample 08JW691, the Triassic sill, and the tuff (Sample 08JW534) from the Upper Inskip Formation were exposed to the entire deformation. This gives a maximum age for the timing of deformation of Early Triassic. More analysis of the other deformed sills/dikes in the area is necessary to more narrowly constrain the timing of the deformation.

The first phase of deformation (D_1) is recorded in the angular unconformable relationship between the Upper/Lower Inskip Formation and the Rochester Member Rhyolite. Timing of deformation occurred after the deposition of the Upper Inskip

Formation, which is interpreted to be Early Triassic based on the deposition of a tuff (Sample 08JW534), which yielded an age of 249.08 Ma. The period of tilting and erosion occurred before the deposition of the Rochester Member of the Koipato Group, which has also been assigned an age of Early Triassic.

Golconda Thrusting along the contact between the Lower Inskip Formation and the Valmy Formation represents the second phase of deformation (D_2). The thrust emplaced the Upper and Lower Inskip Formation as well as the Rochester Member in the hanging wall over the Valmy Formation. Along the northern trace of the thrust in the East Range, the Rochester Member and Valmy Formation are juxtaposed by the fault. This relationship of the thrust cutting the Early Triassic Rochester Member provides the maximum age constraint for the thrust. A late Middle Jurassic granodiorite pluton (Sample 09JW891, age 161.86 Ma) cross-cuts the thrust contact between the Inskip Formation and Valmy Formation, providing a minimum age for Golconda thrusting. The Golconda allochthon is interpreted to have been thrust from west-to-east over rocks of the Roberts Mountains allochthon and its overlap sequence along the Golconda Thrust. East-directed movement is also interpreted here for conformity with previous interpretations.

D_3 is documented by a penetrative deformation that produced foliation, transposed bedding, and formed a stretching lineation. Formation of the penetrative foliation may have coincided with the intrusion of late Middle Jurassic plutons, such as the granitic pluton that cores the domal structure near Lee Peak. As the pluton intruded, the foliation formed a west-directed sense of shear while accommodating space for the pluton. Sample 08JW462 is a sill that has been penetratively deformed and is approximately the same thickness and has the same mineral composition as a nearby sill (Sample 08JW661),

which was not deformed. Because Sample 08JW462 is penetratively deformed and has zircon data ranging from 162 Ma and 164 Ma, it appears older than the undeformed sills/plutons. D_3 deformation may have happened within a few million years between the penetratively deformed sill (Sample 08JW462, at 162-164 Ma) and the intrusion of the undeformed sill (Sample 08JW661, at 161.80 Ma).

Deformation from the fourth phase (D_4) resulted in map-scale folding produced by east-west contraction. Because D_4 folds affected the penetrative foliation, the timing of folding is constrained between the age of D_3 foliation and the undeformed late Middle Jurassic sill. In the central East Range, the folding is expressed in a northeast trending anticline, which is cored by a Jurassic pluton. The western limb of the anticline is at a high angle and may represent a top to the west vergence for the folding. East verging outcrop scale folds may be parasitic to the larger structure and developed at the same time.

The fifth phase of deformation (D_5) is recognized by outcrop-scale folding ($D_{4\text{-}5}$ folds) with a top to the east vergence and by development of a crenulation cleavage. The D_3 penetrative foliation was folded along the western limb of the anticline. A minimum age for the folding comes from the undeformed sill (Sample 08JW661) dated at 161.80 Ma. The maximum age of D_5 is constrained to after the earlier forms of deformation. $D_{4\text{-}5}$ deformation is similar to deformation caused by the Fencemaker Thrust system identified in other localities like Blue Mountain and the Santa Rosa Range (Wyld, 2002). In this study, $D_{4\text{-}5}$ deformation is interpreted to have been formed during Fencemaker thrusting.

Table 2: Deformational History and Timing Interpretation

Phase	Products of Deformation	Timing Interpretation
D_5	Outcrop-scale folding Crenulation cleavage (east-directed movement)	Contrained to late middle Jurassic before intrusion of undeformed sill at 161.80 Ma
D_4	Map-scale folding (antiform trending northeast-southwest through north-central East Range) (west-directed movement)	late Middle Jurassic
D_3	Formation of the penetrative foliation (west-directed movement)	Interpreted to have formed during emplacement of late Middle Jurassic plutons
D_2	Golconda Thrust between the Lower Inskip and the Valmy Formation (east-directed movement)	After Early Triassic deposition of the Rochester and before cross cutting pluton 161.86 Ma (late Middle Jurassic)
D_1	Angular Unconformity between Rochester member of the Koipato group and the Inskip	Between 249.04 Ma (Early Triassic) and Early Triassic deposition of the Rochester

Structural Interpretations

Based on field and map relationships, the Lower Inskip Formation/Valmy Formation contact is reinterpreted as a thrust fault with the Lower Inskip Formation thrust over the Valmy Formation. Slickensides are abundant (Figure 16) at the contact between the formations, and not present throughout the rest of the Inskip Formation or the Valmy Formation. These slickenlines have been folded, so the timing of the faulting is prior to the fourth phase of deformation and is interpreted to have resulted during the second phase of deformation. Speed et al. (1988) described the upper Paleozoic formations of the east range as having been transported from the east into their current position as the Willow Creek allochthon. This west-directed movement may have resulted in the formation of the west-directed microstructures and formation of the penetrative foliation observed in the Upper and Lower Inskip Formation. This would place the timing of the thrusting after the deposition of the Upper Inskip Formation and before the emplacement of the pluton (Sample 09JW891) that stitches the contact between the Upper and Lower Inskip Formation and the Lower Inskip Formation with the Valmy Formation. This constrains the timing of emplacement to between the Early Triassic and the late Middle Jurassic. In this case, the Upper Inskip Formation (Koipato Group) rode in piggyback to its current location. Map relationships also show the fault to cut the rocks that are mapped as Rochester Member Rhyolite on the eastern side of the East Range just to the north and east of the Rockhill Canyon area, which additionally indicates a post-Early Triassic age of thrusting.

Although west-directed thrusting is plausible and expressed in the Sonoma Range to the east of the East Range, this is not the only possible interpretation for the west-directed microstructures seen in the Inskip Formation. Top to the west structures may have been the result of space accommodation by the Inskip Formation for the large granodiorite pluton that intruded near Lee peak at the center of the domal structure present on the eastern side of the East Range. Strain in the wall rocks surrounding this intrusion could have produced the penetrative foliation throughout the Inskip Formation. Age constraints are few for the pluton but Speed et al. (1988) reported a K-Ar cooling age of 151 Ma. Non-to slightly deformed sills from this study place a minimum age for deformation at 161.86 +/- 0.044 Ma. Because the K- Ar age reported likely represents a cooling age, it may be some what younger than the deformation. If the penetrative foliation formed during emplacement of the pluton, and did not accompany the thrusting on the fault between the Valmy Formation and Lower Inskip Formation, then the penetrative foliation likely has obscured older structures related to the thrusting. Movement on the thrust could have been either west or east-directed. Rootless isoclinal folding (Figure 21) in the Upper Inskip Formation is east-directed. More precise dating of the pluton is needed to evaluate its timing relationship to deformation.

Another possibility is that thrusting of the Lower and Upper Inskip Formation over the Valmy Formation caused little or no deformation in the overriding plate. The Limerick Member in the Humboldt Range has very little penetrative deformation even though the Fencemarker Thrust is in closer proximity to the Humboldt Range than it is to the East Range. In this scenario, the thrusting (D_2) could have originated from either direction while leaving little penetrative deformation. Then, penetrative foliation (D_3) and

the folding (D_4-D_5) possibly related to Fencemaker thrusting could have over-printed any of the earlier features. Golconda thrusting traditionally has been considered as propagating from the west to the east. Therefore, the author favors top to the east-directed thrusting during D_2 for the emplacement of the Lower and Upper Inskip Formation. If the thrusting is Jurassic in age, then the Golconda Thrust may be part of the Fencemaker thrust system and the two thrusts might sole into the same basal thrust at depth.

One of the major objections to the interpretation of the Valmy Formation and the Lower Inskip Formation being in fault contact is that the bedding of each of the formations appears to be parallel on both sides of the contact for much of the length of the contact. However, thrust faults commonly follow a ramp/flat geometry and the resulting parallel bedding along the contact could have resulted during a "flat" segment of the thrusting. Near the northern end of the thrust strand, where it becomes the contact between the Havallah sequence and the Valmy Formation, the thrust cuts through the Havallah sequence and up into the Rochester Member. This part of the thrust could be considered a hanging wall ramp. Additionally, penetrative deformation and foliation development (D_3) may have transposed original bedding in some places, creating a sub-parallel geometry. This sub-parallel relationship may have masked the angularity of the bedding and the nature of the contact as a fault.

The timing of late Middle Jurassic for the waning of the deformation coincides with the time of Luning-Fencemaker thrusting. Although the Luning-Fencemaker thrust system doesn't pass through the central East Range, it does outcrop approximately 10 miles away in the far north-western extent of the range. Therefore, the north-central East Range may have been affected by the Luning-Fencemaker fold and thrust belt and

deformation propagating into the footwall of the Fencemaker Thrust. Outcrop scale folding described in this study shows a southeast vergence while other studies of deformation from the Luning-Fencemaker fold and thrust belt also show a top to the southwest direction of folding (Oldow et al., 1984). Rocks in the Santa Rosa Range to the north of the East Range also exhibit a second phase of folding and development of a crenulation cleavage after the phase of deformation that produced the first set of folds. This phase in the Santa Rosa Range is thought to have been caused by northeast to southwest contraction (Wyld, 2002). In the rocks of the north-central East Range, deformation resulting from D_4-D_5 appears to be similar and may have been coeval to the deformation in the Santa Rosa Range during Fencemaker thrusting.

Regional Implications

With the new correlations of the Upper Inskip Formation as the Limerick Member of the Koipato Group and the Lower Inskip Formation as an undesignated facies of the Havallah sequence, the field relationships of the north-central East Range are similar to the relationships that exist near China Mountain in the northern Tobin Range, where the Sonoma Orogeny was first described by Silberling and Roberts (1962). Upper Paleozoic Havallah basinal rocks were emplaced along the Golconda Thrust over the Lower Paleozoic rocks of the Roberts Mountains allochthon and the Antler Overlap Sequence. These rocks were overlain unconformably by the Koipato Group. However, nowhere does the Koipato Group lay unconformably on the Lower Paleozoic rocks of the Antler allochthon or the overlap sequence. Because similar field relationships exist in the north-

central East Range, the thrust following the contact between the Lower Inskip Formation and the Valmy Formation may be an extension of the Golconda Thrust. Regional structures show an antiform extending through the center of the north-central East Range and plunging to the southwest. Previous interpretation (Stahl, 1987) has traced the Golconda thrust along the southeast limb of the antiform (Figure 38), yet it has not been previously interpreted to extend to the northwest limb of the antiform. Reinterpretation of the contact of the Lower Inskip Formation and the Valmy Formation as a thrust allows correlation with the Golconda Thrust, and it would occupy the correct structural and tectono-stratigraphic position on the west limb of the dome (Figure 39).

Previous work has linked the Winnemucca Fold and Thrust Belt of the northern Sonoma Range to the Willow Creek Thrust (Figure 38) (Stahl, 1987). The new interpretation of the thrust following the Lower Inskip Formation/Valmy Formation contact in the East Range as the Golconda Thrust results in a reversal of thrust orientation from the work by Stahl (1987). This study has the entire Inskip Formation and the Rochester Member Rhyolite in the hanging wall of the thrust over the Valmy Formation, whereas the earlier study (Stahl, 1987) has the Inskip Formation and the Valmy Formation in the hanging wall and the Rochester Member in the footwall. The footwall rocks in the Sonoma Range are interpreted to be Triassic shelf deposits. This change in thrust relationships between the two ranges may be due to a back-breaking thrust in the northern Sonoma Range, which occurred during thrusting as a way to accommodate space. However, the relationship between the Winnemucca Fold and Thrust Belt and the Golconda Thrust has not been studied and analyzed in detail by this study, and the Winnemucca Fold and Thrust Belt may still represent a west-directed system that could

be more recent than the Golconda Thrust in the East Range. If the Golconda Thrust and the Winnemucca Fold and Thrust Belt are concurrent, then the implications for the Golconda Thrust being a Jurassic feature are more convincing. Additional work is required to determine the relationship and timing of the two thrusting events.

Interpretation of the Upper Inskip Formation as a facies of the Limerick Member (part of the Koipato Group) expands the known distribution of the Limerick Member to the East Range instead of only residing in the Humboldt Range. The Limerick Member may represent a more wide-spread formation than previously thought.

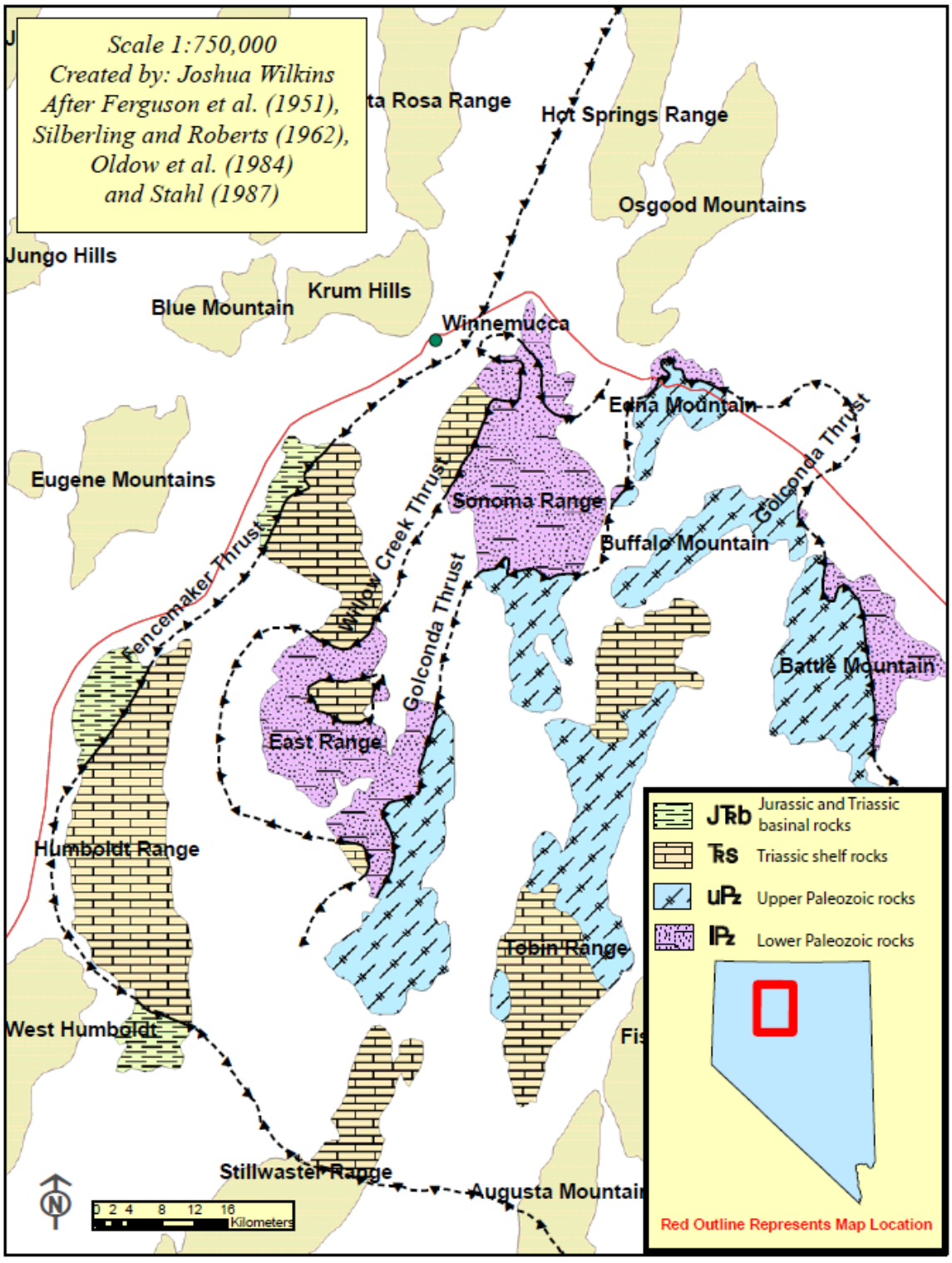

Figure 38. Previous Interpretation of the Golconda and Willow Creek Thrusts.

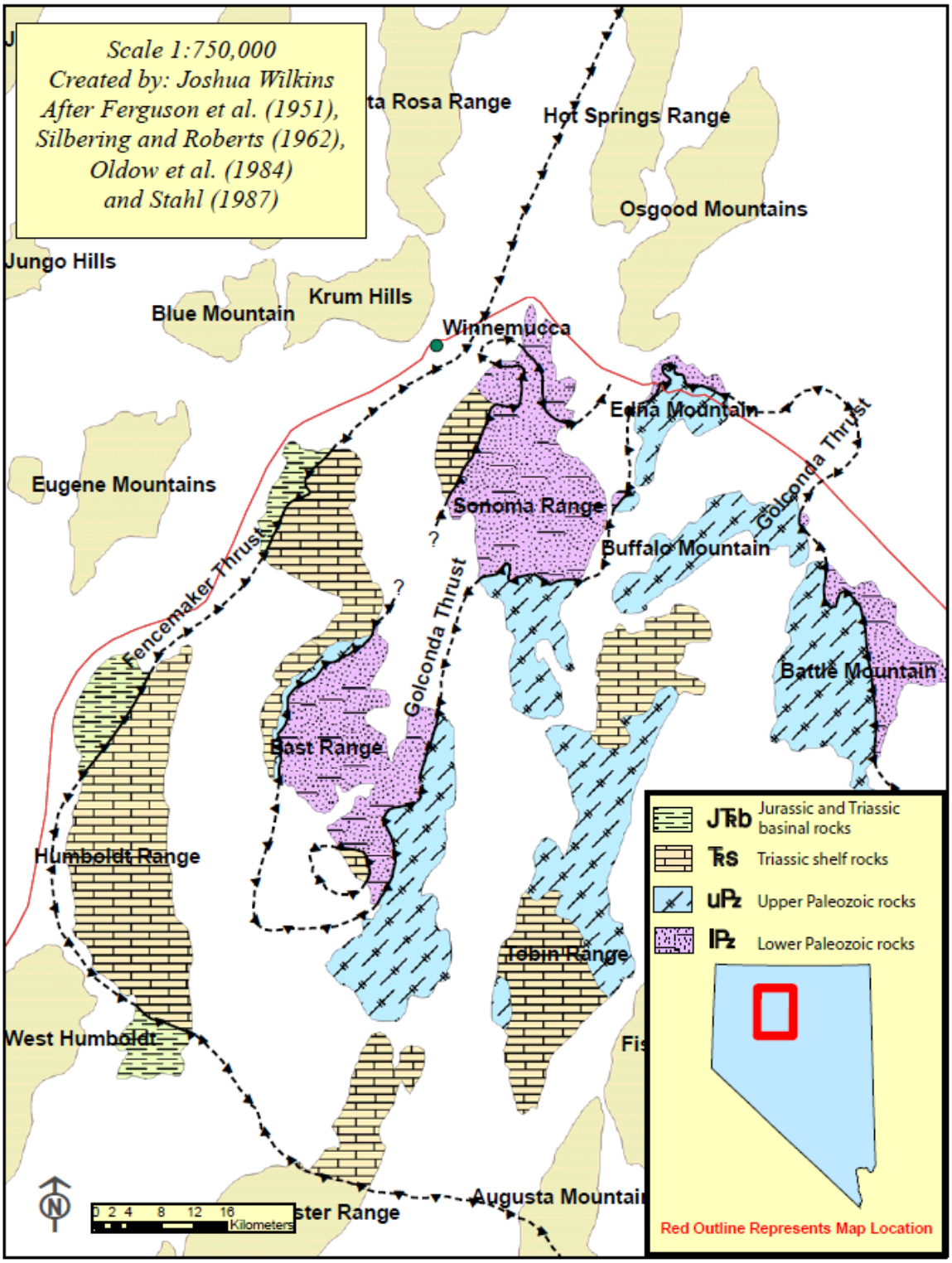

Figure 39. New Interpretation of the Golconda Thrust from This Study.

CONCLUSIONS

New U-Pb zircon geochronology sampled from volcanic layers, intrusive sills, and a small pluton yielded ages that build upon previous interpretations as well as considerably change the significance and understanding of the Inskip Formation and the north-central East Range in relation to timing of Mesozoic tectonics.

The Lower Inskip Formation is reinterpreted to be structurally above the lower Paleozoic Valmy Formation (Silberling and Roberts, 1962; Hargett, 2002). Fossil ages and lithostratigraphy are similar to that of the Havallah sequence and the Lower Inskip Formation is reinterpreted to correlate with the Havallah sequence (Ferguson et al., 1951; Silberling and Roberts, 1962; Ketner et al., 2000), differing from previous attempts at correlation by including only the Lower Inskip Formation rather than the entire Inskip Formation. By assigning the Lower Inskip Formation to the Havallah sequence, map relationships juxtapose Lower Inskip Formation and Havallah sequence along strike across what has been interpreted to be the Willow Creek Thrust. This relationship requires readjustment for the placement of the thrust, which may follow the structural contact between the Valmy Formation and the Lower Inskip Formation.

Unconformably overlying the Lower Inskip Formation is the Upper Inskip Formation. A U-Pb zircon weighted mean age, obtained from a tuff in the lower half of the Upper Inskip Formation, yielded an Early Triassic age of 249.08 +/- 0.14 Ma. Based

on the new radiometric age and similarity of lithology, the Upper Inskip Formation is correlated to the Limerick Member of the Koipato Group.

Previously, the Rochester Member was thought to be in structural contact with the Inskip Formation across the Willow Creek Fault and to overlie the Havallah sequence in an unconformable relationship (Whitebread, 1978). However, the relationship between the Upper/Lower Inskip Formation and the overlying Rochester Member of the Koipato Group is reinterpreted in this work to be an angular unconformity. Correlation of the Upper Inskip Formation as part of the Koipato Group links it with the Rochester Member Rhyolite both in age and tectonic setting. Both members of the Koipato Group have been interpreted to be Early Triassic in age (Vikre, 1977). The angular relationship is observable on aerial imagery along the western edge of the East Range where the Rochester Member is juxtaposed obliquely next to the Upper Inskip Formation.

A large antiform extends across the central East Range, trending in a northeast-southwest orientation. Along the southern limb of the fold, an interpreted trace of the Golconda Thrust has been mapped, but its potential projection into the northern limb of the fold was not clear (Stahl, 1987). New interpretation from this study extends the trace of the Golconda Thrust to close around the southern end of the antiform and follow the contact between the Lower Inskip Formation and the Valmy Formation. With the new age interpretations and correlations for the Upper and Lower Inskip Formation, relationships in the East Range are similar to those at Golconda Summit where the Golconda Thrust was first described.

At least five phases of deformation occurred in the Upper and Lower Inskip Formation of the East Range. The first phase (D_1) of deformation occurred before the

deposition of the Rochester Member and after deposition of the Upper Inskip Formation, and the timing of this event is constrained to the Early Triassic. Deformation tilted the upper Paleozoic rocks of the East Range and is recognized by the angular unconformity between the Rochester Member and Inskip Formation. The second phase (D_2) formed during Golconda thrusting as it transported the upper Paleozoic rocks of the Lower Inskip Formation and the Triassic Koipato Group over the lower Paleozoic rocks of the Valmy Formation. This fault cross-cuts the Rochester Member Rhyolite and is interpreted to have formed after Early Triassic deposition of the Rochester Member and before late Middle Jurassic plutonism. Next (D_3) formed the penetrative foliation prevalent throughout the area of the central East Range. The penetrative foliation is subparallel to original bedding and has at least local west-directed shear, identified by sigma-type winged porphyroclasts and quarter structures on oriented thin sections. However, evidence for top to the east shear is present as well, including some winged porphyroclasts and tiled feldspar grains. This heterogeneity may represent a pure shear component to the overall bulk deformation. The penetrative foliation is thought to have formed during intrusion of the late Middle Jurassic pluton at the core of the domal structure. The fourth phase (D_4) of deformation is the map-scale folding with a southeast-northwest contractional direction that formed the regional antiform and dome in the central part of the range. Following the formation of the penetrative foliation and the map-scale folding, a southeast directed fifth phase (D_5) of deformation, probably related to Fencemaker thrusting, folded the penetrative foliation with a top to the east vergence and formed a crenulation cleavage (Oldow et al., 1984; Wyld, 2002). Deformation from

the last three phases may have formed during a relatively brief several million year period during the late Middle Jurassic.

New high precision radiometric ages for the Inskip Formation made possible some of the correlations and interpretations for this work. With the correlation of the Upper and Lower Inskip Formation, to the Limerick Member and Havallah sequence respectively, the use of the name Inskip Formation should be abandoned and replaced with the correlative terms.

WORKS CITED

Bartley, J.M., 1990, Structure of the Eureka thrust belt, Nevada: Geological Society of America, Abstracts with Programs 22: 5.

Brueckner, H.K., Snyder, W.S., 1985, Structure of the Havallah sequence, Golconda allochthon, Nevada: Evidence for prolonged evolution in an accretionary prism: Geological Society of America Bulletin 96: 1113-1130.

Burchfiel, B.C., Cowan, D.S., Davis, G.A., 1992, Tectonic overview of the Cordilleran orogen in the western United States: The Geology of North America, The Cordilleran Orogen: Conterminous U.S., The Geological Society of America G-3: 407-479.

Crafford, A.E.J., 2008, Paleozoic tectonic domains of Nevada: An interpretive discussion to accompany the geologic map of Nevada: Geosphere 4: 260-291.

Crowley, J.L., Schoene, B., Bowring, S.A., 2007, U-Pb dating of zircon in the Bishop Tuff at the millennial scale: Geology 35:1123-1126.

du Bray, E.A., 2007, Time, space, and composition relations among northern Nevada intrusive rocks and their metallogenic implications: Geosphere 3: 381-405.

Dunston, J. F., Northrup, C.J., Snyder, W.S., 2001, Post-latest Triassic Thrust Emplacement of the Golconda Allochthon, Sonoma Range, Nevada: Geological Society of America, Abstracts with Programs 33: 327.

Elison, M.W., 1987, Structural Geology and Tectonic Implications of the East Range, Nevada: Northwestern University: Evanston, IL.

Ferguson, H.G., Muller, S.W., Roberts, R.J., 1951, Geology of the Winnemucca quadrangle: Nevada. U. S. Geological Survey, Quadrangle Map GQ-11.

Gehrels, G. E., 2000, Detrital zircon geochronology of the Roberts Mountains allochthon, Nevada: in Soreghan, M. J., and Gehrels, G. E., eds., Paleozoic and Triassic paleogeography and tectonics of western Nevada and northern California: Boulder, Colorado, Geological Society of America Special Paper 347, p. 19-42.

Geissman, J.W., Gillett, S.L., Oldow, J.S., 1990, Preliminary Paleomagnetic Results from the Triassic Prida Formation (Lower Star Peak Group), West-Central Nevada, and Implications for Latitudinal Displacement: Geophysical Reasearch Letters 17: 697-700.

Gerstenberger, H., Haase, G., 1997, A highly effective emitter substance for mass spectrometric Pb isotope ratio determinations: Chemical Geology 136: 309-312.

Hargett, R. N., 2002, The Geology of the Inskip Canyon Area, East Range, Nevada: Boise State University: Boise, ID.

Johnson, M.G., 1977, Geology and Mineral Deposits of Pershing County, Nevada: Nevada Bureau of Mines and Geology, Bulletin 89.

Jones, A.E., 1997, Geologic map of the Hot Springs Peak quadrangle and the southeastern part of the Little Poverty quadrangle, Nevada: Nevada Bureau of Mines and Geology Field Studies Map 14.

Ketner, K.B., 1984, Recent studies indicate that major structures in northwestern Nevada and the Golconda thrust in north-central Nevada are of Jurassic or Cretaceous age: Geology 12: 483-486.

Ketner, K.B., 1998, The Nature and Timing of Tectonism in the Western Facies Terrane of Nevada and California—An Outline of Evidence and Interpretations Derived From Geologic Maps of Key Areas: U.S. Geological Survey Professional Paper 1592.

Ketner, K.B., 2008, The Inskip Formation, the Harmony Formation, and the Havallah Sequence of Northwestern Nevada—An Interrelated Paleozoic Assemblage in the Home of the Sonoma Orogeny: U.S. Geological Survey Professional Paper 1757, 21 p.

Ketner, K.B., Wardlaw, B.R., Harris, A.G., Repetski, J.E., 2000, The East Range, Norhtwestern Nevada: a Neglected Key to the Tectonic History of the Region: In Cluer, J. K., Price, J. G., Struhsacker, E. M., Hardyman, R. F., and Morris, C. L., eds., 2000, Geology and Ore Deposits 2000: Symposium Proceedings, Geological Society of Nevada, 1: 397-418.

Krogh, T.E., 1973, A low contamination method for hydrothermal decomposition of zircon and extraction of U and Pb for isotopic age determination: Geochimica et Cosmochimica Acta 37:485-494.

Maher, K.A., Saleeby, J., 1988, Age constraints on the geologic evolution of the Jackson Mountains, NW Nevada: Geological Society of America Abstracts with Programs 20: 177.

Mattinson, J.M., 2005, Zircon U-Pb chemical abrasion ("CA-TIMS") method: combined annealing and multi-step partial dissolution analysis for improved precision and accuracy of zircon ages: Chemical Geology 220:47-66.

Oldow, J.S., Ave Lallemant, H.G., Schmidt, W.J., 1984, Kinematics of Plate Convergence Deduced from Mesozoic Structures in the Western Cordillera: Tectonics 3: 201-227.

Poole, F.G., Sandberg, C.A., 1977, Mississippian paleogeography and tectonics of the western United States, in Stewart, J.H., Stevens, C.H., Fritsche, A.E., eds., Paleozoic paleogeography of the western United States: Los Angeles, Califonia, Pacific Section, Society of Economic Paleontologists and Mineralogists Pacific Coast Paleogeography Symposium I, 67-85.

Roberts, R.J., 1964, Stratigraphy and structure of the Antler Peack quadrangle, Humboldt and Lander Counties, Nevada: U.S. Geological Survey Professional Paper 459-A.

Roberts, R.J., Hotz, P.E., Gilluly, J., Ferguson, H.G., 1958, Paleozoic Rocks of North-Central Nevada: AAPG Bulletin 42: 2813-2857.

Saleeby, J.B., Busby-Spera, C., 1992, Early Mesozoic tectonic evolution of the western U.S. Cordillera: The Geology of North America, The Cordilleran Orogen: Conterminous U.S., The Geological Society of America G-3: 107-168.

Schmitt, J.G., 1989, Tectonic setting of Cretaceous intermontane basins within the hinterland of the Sevier orogenic belt, east-central Montana: Geological Society of America Abstracts with Programs 21: 140-141.

Schmitz, M.D., Schoene, B., 2007, Derivation of isotope ratios, errors and error correlations for U-Pb geochronology using ^{205}Pb-^{235}U-(^{233}U)-spiked isotope dilution thermal ionization mass spectrometric data: Geochemistry, Geophysics, Geosystems (G^3) 8, Q08006, doi:10.1029/2006GC001492.

Schweickert, R.A., Snyder, W.S., 1981, Paleozoic Plate Tectonics of the Sierra Nevada and Adjacent Regions: In Ernst, W. G. Ed., The Geotectonic Development of California, 182-201. Englewood Cliffs, N. J.: Prentice-Hall, Inc.

Speed, R.C., 1977, Island-arc and other Paleogeographic Terranes of Late Paleozoic Age in the Western Great Basin: In Stewart, J. H., Stevens, C. H., and Fritsche, A. E. Ed., Paleozoic Paleogeography of the Western United States, The Pacific Section Society of Economics Paleontologists and Mineralogists, Pacific Coast Paleogeography Symposium 1: 349-362.

Speed, R.C., Elison, M.W., Heck, F.R., 1988, Phanerozoic Tectonic Evolution of the Great Basin: In Ernst, W.G. Ed., Rubey Volume 7: 573-605.

Speed, R.C., Silberling, N.J., 1989, Field Trip Guidebook T122, Early Mesozoic Tectonics of the Western Great Basin, Nevada: American Geophysical Union, Washington D.C.

Silberling, N.J., Roberts, R. J., 1962, Pre-Tertiary Stratigraphy and Structure of Northwestern Nevada: Geological Society of America, Special Paper 72, 1-58.

Silberling, N.J., Wallace, R.E., 1969, Stratigrpahy of the Star Peak Group (Triassic) and overlying Mesozoic rocks, Humboldt Range, Nevada: U.S. Geological Survey Professional Paper 592. 50 p.

Snyder, W.S., Brueckner, H.K., 1983, Tectonic Evolution of the Golconda Allochthon, Nevada: Problems and Perspectives: In Stevens, C. A., Ed., Pre-Jurassic Rocks in Western North American Suspect Terranes: The Pacific Section Society of Economics Paleontologists and Mineralogists 32: 103-123.

Snyder, W.S., Brueckner, H.K., 1989, Permian-Carboniferous tectonics of the Golconda Allochthon; an accreted terrane in the Western United States: Compte Rendu 4 – XI Congres International de Stratigraphie et de Geologie du Carbonifere: 294-312.

Stacey, J.S., Kramers, J.D., 1975, Approximation of terrestrial lead isotope evolution by a two-stage model: Earth and Planetary Science Letters 26:207-221.

Stahl, S.D., 1987, Mesozoic structural features in Sonoma Canyon, Sonoma Range, Humboldt and Pershing counties, Nevada: GSA Centennial Field Guide—Cordilleran Section: 85-90.

Steiger, R.H., Jager, E., 1977, Subcommission on geochronology: convention on the use of decay constants in geo- and cosmochronology: Earth and Planetary Science Letters 36:359-362.

Vikre, P.G., 1977, Geology and silver mineralization of the Rochester district, Pershing County, Nevada, Ph.D. thesis: Stanford Univ., 404 p.

Whitebread, D.H. 1978, Preliminary Geologic map of the Dun Glen quadrangle, Pershing County, Nevada: U. S. Geological Survey Open File Report 78-407, 1:48,000.

Whitebread, D.H. 1994, Geologic map of the Dun Glen quadrangle, Pershing County, Nevada: U. S. Geological Survey Miscellaneous Investigations Map I-2409, scale 1: 48,000.

Wyld, S.J., 2002, Structural evolution of a Mesozoic backarc fold-and-thrust belt in the U.S. Cordillera: New evidence from northern Nevada: GSA Bulletin 114: 1452–1468.